Master's thesis

NTNU
Norwegian University of Science and Technology
Faculty of Economics and Management
Department of Economics

Olav Yoo Stavheim Rudberg

Electricity Price and Volatility

The Effect of Rainfall and Temperature

Master's thesis in Economics
Supervisor: Colin Green (NTNU)
Co-supervisor: Jørgen Bjørndalen (DNV)
May 2022

NTNU
Kunnskap for en bedre verden

DNV

Olav Yoo Stavheim Rudberg

Electricity Price and Volatility

The Effect of Rainfall and Temperature

Master's thesis in Economics
Supervisor: Colin Green (NTNU)
Co-supervisor: Jørgen Bjørndalen (DNV)
May 2022

Norwegian University of Science and Technology
Faculty of Economics and Management
Department of Economics

NTNU

Kunnskap for en bedre verden

Preface

Finally! It has been completed! This dissertation is the completion of a 2-year MSc in Economics, and 5-years studying economics at the Norwegian University of Science and Technology (NTNU). Definitely hard and frustrating, but rewarding in the end.

I would like to thank my supervisors Colin Green at NTNU and Jørgen Bjørndalen at DNV for insightful discussions, knowledge, and guidance on a challenging subject. Thank you to my mother, father and sister for the support during my studies in Economics, Tim for proofreading, and my girlfriend Hanna. Lastly, I have to thank everyone up on the 5th floor and Simon for listening to all problems that arose during the writing process.

Disclaimer

I hereby declare that this dissertation is my own original work. Sources used are acknowledged and cited in the bibliography section. Mistakes and opinions are my own.

Olav Yoo Stavheim Rudberg , Trondheim, 31.05.2022

Table of Acronyms

Acronym	Description
MWh	Megawatt hour
AR	Autoregressive
MA	Moving Average
ARMA	Autoregressive moving average
ARIMA	Autoregressive integrated moving average
ARCH	Autoregressive conditional heteroskedasticity
GARCH	Generalized autoregressive conditional heteroskedasticity
EGARCH	Exponential generalized autoregressive conditional heteroskedasticity
NVE	The Norwegian Water Resources and Energy Directorate
HBV-model	Hydrologiska Byråns Vattenbalanssektions modell
DF	Dickey Fuller
ADF	Augmented Dickey Fuller
MS	Markov-Switching
MAE	Mean absolute error
MAPE	Mean absolute percentage error
MSE	Mean squared error
RMSE	Root mean squared error
AIC	Akaike information criterion
BIC	Schwartz bayesian information criterion
ACF	Autocorrelation function
PACF	Partial autocorrelation function
LF, LLF, LL	Likelihood function, logarithmic likelihood function, logarithmic likelihood
MISO	Midwest Independent System Operator
EEX	European Energy Exchange AG
APX	Amsterdam Power Exchange

Abstract

Research on electricity price and volatility has previously been conducted, but few studies include effects that are probable to affect electricity prices and volatility. This dissertation studies the system price at Nord Pool from week 1 2008, through week 52 2021. Autoregressive integrated moving average (ARIMA) and general autoregressive conditional heteroskedasticity (GARCH) models are used separately, and jointly as ARIMA-GARCH models to predict the system price and volatility. Seasonally adjusted and population weighted temperature and rainfall for 6 Norwegian cities is included. Rainfall captures additional expectations and supply effects alongside rainfall, whereas temperature captures additional consumption and demand effects alongside temperature. Water magazine deviation, wind power production, and the sum of snow, surface and ground water in Norway is included. The effects consumption, demand and temperature have in contribution to explaining the system price and volatility are found to be small. The effects expectations, supply and rainfall have on the system price are found to be ambiguous, but the effects do somewhat contribute to explaining the system price and volatility. The dissertation finds evidence of quarterly and half-year seasonal effects within the modeling process. Results for the system price indicate exponential volatility persistence. An unrestricted model including both temperature and rainfall is the most persistent, and excluding rainfall is less persistent than excluding temperature. A model without rainfall reacts less to shocks in volatility than a model without temperature, however the correlation in variance over 2 periods is lower. Wind power production, sum of snow, ground, and surface water, including magazine deviation have a statistically significant and negative effect on the system price. A highly autoregressive system price of order 1 is found.

Sammendrag

Studier av elektrisitetspriser og volatilitet har tidligere blitt gjennomført, men få studier inkluderer effekter som potensielt påvirker elektrisitetspriser og volatilitet. Masteravhandlingen studerer nordisk systempris fra Nord Pool fra uke 1 2008, ut uke 52 2021. Autoregressive integrated moving average (ARIMA) og general autoregressive conditional heteroskedasticity (GARCH) modeller benyttes separat og sammenslått som ARIMA-GARCH modeller for å predikere systempris og volatilitet. Sesongjustert og befolkningsvektet temperatur og nedbør for 6 byer i Norge benyttes. Nedbør fanger opp forventnings- og tilbudseffekter i tillegg til nedbør. Temperatur fanger opp konsum- og etterspørselseffekter i tillegg til temperatur. Magasinavvik, vindenergiproduksjon og summen av snø-, mark-, og grunnvann inkluderes som kontrollvariabler. Avhandlingen finner at effektene av konsum, etterspørsel, og temperatur på systemprisen og volatilitet er små. Videre er effektene av forventning, tilbud og nedbør på systempris tvetydige, men bidrar til å forklare systempris og volatilitet. Avhandlingen finner bevis for kvartals- og halvårseffekter. Estimeringsresultater indikerer en eksponentiell volatilitetspersistens hvor en fullspesifisert modell med temperatur og nedbør har høyest persistens. Restriksjoner på nedbør gir lavere volatilitetspersistens enn restriksjoner på temperatur. Estimering uten nedbør gir lavere volatilitetsrespons fra sjokk enn estimering uten temperatur, med lavere korrelasjon i varians over 2 perioder. Vindenergiproduksjon, magasinavvik og sum av snø-, mark-, og grunnvann har en statistisk signifikant og negativ effekt på systemprisen. Avhandlingen finner i tillegg bevis for en svært autoregressiv prosess av 1 orden.

Contents

1 Introduction

Electricity prices are subject to high volatility. Between 2008 and 2021 weekly system prices for electricity at Nord Pool varied between 1.6600€/MWh[1] and 201€/MWh. Electricity prices are affected by multiple effects which contribute to volatility. For instance, Norway is a hydropower dependent nation with 347 hydropower production plants producing around 90% of Norwegian power production, and around 1/6 of global hydropower production (Statkraft, 2022). Hydropower is affected and determined by climate, resulting in dependence on rainfall, snowfall, temperature, seasonality, and seasonal consumption patterns, which in turn affects water magazine levels and electricity prices. National water magazine levels are determined directly by rainfall and indirectly by other effects that affect influx to water magazines. Electricity prices surge when water magazine levels are low, for instance in 2021, and vice versa, contributing to electricity prices subject to periods of both highly positive and negative volatility. Furthermore, electricity prices are affected by additional effects like seasonality, production of other energy sources and imports and exports.

A range of studies have been conducted of electricity prices and electricity price volatility across several countries. Different methods have been applied, including artificial intelligence (AI) neural networks, fundamental models, and statistical time series models. Within the statistical time series framework, numerous studies on electricity prices and volatility have been conducted using generalized autoregressive conditional heteroskedasticity models (GARCH) and autoregressive moving average processes (ARMA), often combined into ARMA-GARCH models. For instance, Frömmel et al. (2014) apply a realized GARCH model, Liu and Shi (2013) apply different ARMA-GARCH-M models, while Koopman et al. (2007) apply a REG-ARFIMA-GARCH model to study electricity prices and volatility. While these papers contribute to explaining electricity price and volatility, few studies found by the author explicitly model additional effects which contribute to explain electricity prices and electricity price volatility.

This dissertation studies effects that affect electricity prices and volatility at Nord Pool

[1]MWh = Megawatt hour

from week 1 2008, through week 52 2021, extending available research on electricity price and volatility. An unconstrained, theoretical electricity price, the system price for the Nordic region is used, however the dissertation concentrates on the Norwegian market for simplicity and parsimony when fitting ARIMA and ARIMA-GARCH models. Effects known to affect electricity price and volatility are included, pooled into national effects. These include Norwegian water magazine deviation, influx to water magazines through the sum of snow, ground, and surface water, and Norwegian wind power production. Furthermore, the dissertation examines other effects with regional rainfall and temperature as the prime focus. Rainfall and temperature from 6 Norwegian cities on a weekly frequency are utilized and seasonally adjusted. The cities included are Bergen, Kristiansand, Oslo, Stavanger, Trondheim and Tromsø studied from week 1 2008, through week 52, 2021. Temperature and rainfall are assigned population weights to capture expectation, supply, consumption, and demand effects, in addition to temperature and rainfall effects. To the authors knowledge there are no studies of equal extension. These effects are, however, important both due to potential changes in external effects such as climate both on a regional and national level, and to explain changes in volatility as observed in 2020 and 2021, affecting the system price.

Initially, I use a class of autoregressive integrating moving average models (ARIMA) with emphasis on determining a preferred model specification and population weights through the Box-Jenkins 3-step approach alongside an in-sample system price fit. Subsequently the ARCH and GARCH framework is appended onto the ARIMA framework to study volatility and system price through a restriction-based approach. This includes models with all effects included, and imposed restrictions on rainfall and temperature to better understand how seasonally adjusted and population weighted temperature and rainfall affect volatility and system price. The dissertation has the following thesis statements:

1. To what extent does population weighted and seasonally adjusted temperature and rainfall affect system price and volatility?
2. Which other effects affect system price and volatility?

1.1 Contents

The rest of the dissertation is divided into 5 sections. In section 2, relevant literature is reviewed. First, a broad overview of the most relevant and current literature relevant for the dissertation is described before a more comprehensive revision of 3 papers relevant for the analysis is presented. In section 3, the dataset utilized in the dissertation is presented alongside an introduction to the dataset. Variables in the dataset are stated, including relevant descriptive statistics and a review of data preparation through unit-root tests. Section 4 presents the theoretical framework used in the dissertation. A simplified mathematical assessment of ARMA, ARIMA, ARCH and GARCH models is provided. Furthermore, model selection and information criteria are presented, including a simplified summary of maximum likelihood estimation and model-fit evaluation. Results are presented in section 5. This includes fitting the preferred ARIMA model through the 3-step Box-Jenkins approach, determination of population weights and in-sample fit. Afterwards, a range of ARIMA-GARCH models are estimated with restrictions to seasonally adjusted temperature and rainfall. Robustness is examined, before results are evaluated and discussed. Lastly, a conclusion is given in section 6.

2 Theory and Literature Review

This section presents a broad overview of relevant literature before reviewing the 3 most relevant research papers for the dissertation. Electricity prices are complex, and reviewing a selection of articles is therefore suitable for the subject. This approach has been chosen to deepen understanding and insight of the thesis statement.

2.1 Broad Overview

There exist various relevant research papers on price and volatility for the electricity market in different countries. In general, there are 3 main classes of study. Artificial intelligence (AI) neural networks, fundamental models, and statistical time series models. Within time series modeling of electricity price and volatility, electricity prices are often log-transformed beforehand to simplify interpretation and obtain stationarity (Schlueter, 2010). The most

widespread models for volatility are the (general) autoregressive conditional heteroskedasticity (GARCH and ARCH) models. Furthermore, autoregressive integrated moving average (ARIMA) models are also widely used, often together with GARCH models. For instance, Cifter (2013) log-transforms electricity price returns before estimating different GARCH variants, including a Markov-switching GARCH. Koopman et al. (2007) apply log-differenced daily spot electricity prices with explanatory variables in a REG-ARFIMA-GARCH model on the Nord Pool spot market and several other European power markets. Efimova and Serletis (2014) investigate crude oil, natural gas, electricity price and volatility using both univariate and multivariate GARCH models, while Liu and Shi (2013) estimate 10 different ARMA-GARCH(-M) models. Furthermore, Bowden and Payne (2008) estimate an ARIMA, ARIMA-EGARCH and an ARIMA-EGARCH-M model on 5 MISO hubs with both an in-sample fit and an out-of-sample forecast, while Frömmel et al. (2014) forecast daily electricity price volatility by applying a realized GARCH model.

2.2 Detailed Literature Review

2.2.1 Liu and Shi (2013): Applying ARMA–GARCH Approaches to Forecasting Short-Term Electricity Prices

Liu and Shi (2013) forecast hourly day-ahead electricity prices by estimating a range of ARMA-GARCH models. The research paper falls into the category of statistical time series and applies hourly real time location based marginal prices (LMP) from the ISO New England Market from 1.1.2008 to 28.2.2010 and includes 18.960 observations. Within the time period, the LMP exhibits extreme price spikes and visual evidence of volatility clustering, further emphasized by reported descriptive statistics. Minimum LMP equal 0 and maximum LMP equal 403.23 with an average LMP of 61.09 and a standard deviation of 33.4735, reported in $/MWh. Similar behaviour has also been observed Schlueter (2010) for the EEX Phelix Peak Load Index, the Nord Pool Spot Index, the APX Power UK Industrial Peak Load Index and the APX Dutch Power Peak Load index between 2005 and 2009.

Moreover, electricity prices within the dataset are positively skewed and leptopkurtic. Liu and Shi (2013) highlight that non-normally distributed electricity prices are common in elec-

tricity prices. Since the aforementioned non-normal behaviour is similar to other electricity markets, it is argued that results can possibly be applied as general guidance for other electricity markets. For instance, Nord Pool day-ahead daily system prices from 1.1.2017 until 31.12.2021 exhibit similar behaviour[2].

Liu and Shi (2013) apply the first 2 years of data to fit different ARMA-GARCH(-M) models, while remaining observations are used out-of-sample to test the prediction accuracy of the fitted models. The estimated GARCH models are SGARCH, QGARCH, GJRGARCH, EGARCH and NGARCH. ARMA-GARCH models are fitted for the first 5 models with AR lags 1, 11, 24, 48, 72, 96, 120, 144, 168, 216, 264, 336, 504, 672 and 840, and MA lags 1 to 10, revealing a complex lag-structure. Reported results are all statistically significant at a 0.1% level, which implies daily, weekly, and monthly periodicities or seasonality in electricity prices. Furthermore, results from ARCH(1) and GARCH(1) reports statistically significant time varying volatility. The sum of SGARCH, QGARCH and EGARCH parameters are > 1, indicating exponential volatility persistence. Results from NGARCH, QGARCH, EGARCH and GJR-GARCH indicate nonlinear and asymmetric volatility, previously found for instance by Bowden and Payne (2008) who estimate an ARIMA-EGARCH(1,1) and an ARIMA-EGARCH-M for the Midwest Independent System Operator (MISO) in the United States.

Adjusted R^2, F-tests, AIC, and BIC are used to evaluate the fitted models, including partial autocorrelation function (PACF) plots of residuals from model estimation. Results from PACF are found to be consistent. The fitted ARMA-GARCH models are found highly statistically significant with p-values smaller than 0.0001. Results from AIC and BIC indicates that ARMA models with nonlinear and asymmetric GARCH processes have a better potential to model electricity prices. For instance, AIC and BIC values from ARMA-QGARCH are the highest, whereas values from ARMA-NGARCH are the lowest.

All respective p-values are statistically significant with significance levels below 0.1%, with

[2]Author has analyzed data from `https://www.nordpoolgroup.com/Market-data1/data-downloads/historical-market-data2/` in STATA. Skewness: 3.257. Kurtosis: 24.685.

similar results as the 5 previously estimated ARMA-GARCH models. Estimated parameters are highly statistically significant, and electricity prices exhibit daily, weekly, and monthly periodicities or seasonality, including nonlinear and asymmetrical time-varying volatility. These results are similar to Bowden and Payne (2008) who also discover seasonality and time-varying volatility. Furthermore, Liu and Shi (2013) find that volatility of electricity prices can negatively influence mean electricity prices through a statistically significant and negative mean-term which enters through the GARCH-M specification. Adjusted R^2 indicates that the 5 ARMA-GARCH-M models outperform the 5 former ARMA-GARCH models. P-values from F-tests report highly statistically significant results, all below 0.0001. AIC and BIC values are very similar, except from ARMA-SGARCH-M which report the lowest values.

Model performance is compared by utilizing RMSE, MAE, MAPE and TIC. The ARMA-SGARCH and ARMA-GJRGARCH have the best forecasting performance out of the 5 ARMA-GARCH variants. Among the five ARMA-GARCH-M models, the ARMA-SGARCH-M and ARMA-GJRGARCH-M models provides a superiour model fit. When comparing all 10 models against each other, a clearly dominant model cannot be argumented for. However, the ARMA-SGARCH-M may be preferred due to simplicity and robustness, while maintaining satisfactory prediction accuracy. Nevertheless, all estimated models can accurately forecast the electricity prices in-sample. Liu and Shi (2013) mention that further research might include weather as an exogenous variable to capture electricity demand.

2.2.2 Koopman et al. (2007): Periodic Seasonal Reg-ARFIMA–GARCH Models for Daily Electricity Spot Prices

Koopman et al. (2007) focus on daily spot-prices from Nord Pool (Norway) using a REG-ARFIMA-GARCH model framework. In addition, daily spot-prices from EEX (Germany), Powernext (France) and APX (Netherlands) are also analyzed to check the validity of the model in various markets that are less hydropower dependent than Nord Pool. More specifically, dynamic long memory regression models with autoregressive conditional heteroskedastic errors are considered and estimated with log-likelihood maximization.

First and foremost, Koopman et al. (2007) argument for a random walk process within daily spot prices due to 4 effects who follow:

1. Seasonal dependent electricity prices;
2. Mean reversion due to weather dominant effects which affect the spot prices;
3. Jumps and spikes in electricity prices due to storage capacities; and
4. Volatility clustering.

Therefore, electricity prices are transformed into logarithmic first differences.

Koopman et al. (2007) include 2 explanatory variables relevant for the electricity price; daily Norwegian power consumption, dominated by yearly cycles and a weekly consumption pattern, and weekly water magazine filling levels, dominated by yearly cycles. The seasonal length in the paper is determined to be 7, equal to 1 week.

Initially, descriptive statistics reveal different dynamic properties within the EEX, Powernext and APX as opposed to Nord Pool. Koopman et al. (2007) argue that this is due to the dependence on hydropower generation, which depends on long-run weather conditions at Nord Pool, whereas APX, EEX and Powernext relies on different power mixes.

The results from the REG-ARFIMA-GARCH estimation concludes with significant holiday effects in demand with low return to electricity prices on holidays, and high returns thereafter. Interestingly, the periodic AR-polynomial is stable, and the largest inverse root of the characteristic polynomial equal 0.95, indicating a high level of autoregression within electricity prices. Furthermore, holiday effects are statistically significant, including yearly and half-yearly volatility effects. GARCH parameters are on the boundary of the admissible parameter space, exhibiting high persistence within the conditional variance.

In terms of explanatory variables, water magazine filling levels are used as a proxy for supply side effects with both demeaned levels and demeaned weekly differences. Koopman et al. (2007) find that increase in filling levels has a statistically significant, negative effect

on electricity prices without affecting other parameter estimates in any noteworthy fashion. Furthermore, yearly cycles of electricity prices through the conditional mean are replaced by yearly cycles in water magazine filling levels. Interestingly, long-run effects of magazine filling levels and consumption are statistically insignificant and implies no feedback from electricity prices to consumption. However, a significant part of the short-term price movement can be explained by weekly magazine filling levels and daily electricity consumption within the ranges of the Nord Pool market. Finally, there is a strong relationship between electricity prices and consumption in the short-run.

Koopman et al. (2007) do not find evidence of residual serial correlation through a Ljung-Box Q statistic, with limited erratic behaviour and no evidence of non-normal behaviour. Residual diagnostics therefore show a good model fit. When applied to the APX and EEX, model fit is decent, however Koopman et al. (2007) highlight that market specifics should be taken into account to control for different power mixes.

2.2.3 Bowden and Payne (2008): Short Term Forecasting of Electricity Prices for MISO Hubs: Evidence From ARIMA-EGARCH Models

Bowden and Payne (2008) study the Midwest Independent System Operator (MISO) electricity market with 3 time series models, ARIMA, ARIMA-EGARCH and ARIMA-EGARCH-M. 5 MISO-hubs are analyzed in the paper, the Cinergy Hub, First Energy Hub, Illinois hub, Minnesota hub, and the Michigan hub. The paper assesses model fit through in-sample performance, serial correlation, autoregressive conditional heteroskedasticity, and out-of-sample performance. Hourly real time electricity prices are applied, and real time location-based marginal priced are used in the paper between 9.7.2007 to 6.8.2007.

Unlike the system price, the real time market considers physical limitations. Physical schedules and real time offers are therefore included, updated up to 30 minutes prior to the hour. The market clearing price is calculated as in Equation (`BP.1`). Observe that without congestion costs and transmission losses, the market clearing price equals energy costs and therefore represents the system price which gives an identical price across all MISO hubs. With these

costs considered, the market clearing price might differ between the MISO hubs. LMP for the period shows evidence of volatility clustering.

$$
\begin{aligned}
LMP_{jt} &= EnergyC_t + MCC_{jt} - MLC_{jt} \\
LMP_{jt} &= \quad \textit{Market clearing price} \\
EnergyC_t &= \quad \textit{Energy cost at time } t \\
MCC_{jt} &= \ \textit{Marginal congestion costs at time } t \\
MLC_{jt} &= \ \textit{Marginal cost of transmission losses at time } t
\end{aligned}
\tag{BP.1}
$$

To capture ARCH-effects, including possible leverage, or inverse leverage effects, an EGARCH model is appended onto an ARIMA model. The invertibility conditions for seasonal and non-seasonal moving average terms are statistically significant at a 1% level. Furthermore, shocks to electricity prices are statistically significant at a 1% level with coefficients ranging from 0.4148 to 0.5787 across the MISO hubs. The sign effect is also positive and statistically significant at a 1% level with coefficients from 0.0712 to 0.1901 across the MISO hubs, indicating presence of leverage effects, except for the Illinois hub with statistical significance at a 10% level.

Importantly, volatility persistence is statistically significant at a 1% significance level with a coefficient ranging from 0.7718 to 0.7830 indicating a high volatility persistence. The estimated ARIMA-EGARCH model is free of both serial correlation and further autoregressive conditional heteroskedasticity, except for the Minnesota hub. Here, the Ljung-Box-Q statistic for serial correlation is marginally significant at a 10% level.

The third model estimated is an ARIMA-EGARCH-M model, to capture the impact of the conditional volatility of electricity prices on the mean of the respective hourly electricity prices. This is captured through the M-term. Invertibility conditions are satisfied for all hubs, statistically significant at a 1% level. Shocks to electricity prices through the size effect are statistically significant at a 1% significance level, with the coefficient ranging from 0.4145 to 0.5545. Sign effects are positive and statistically significant at a 1% significance level, except for Illinois which is significant at a 10% significance level. The coefficient varies

from 0.0693 to 0.1914, which indicate evidence of an inverse leverage effect.

Furthermore, volatility persistence is statistically significant at a 1% level, with a coefficient from 0.7685 to 0.7835 across the MISO hubs, indicating high volatility persistence. The residuals are free of both serial correlation and autoregressive conditional heteroskedasticity, except for the Minnesota hub where the Ljung-Box-Q statistic is marginally significant at the 10% level.

Bowden and Payne (2008) also assess forecasting performance and model fit. Firstly, an in-sample forecast is completed, generated from the model over the estimation period to assess model behaviour compared to real time electricity prices for each hub. RMSE, MAE, MAPE and Theil's inequality coefficient are used as criteria. MAE and MAPE are lower for certain ARIMA-EGARCH and ARIMA-EGARCH-M models. However, RMSE and Theils inequality coefficient favour the ARIMA model for each hub. Secondly, an out-of-sample dynamic 24 hour forecast on the 6.8.2008 is examined. The ARIMA-EGARCH-M outperforms ARIMA and the ARIMA-EGARCH for Cinergy, First Energy, and the Illinois hub, whereas the ARIMA model dominates in the Michigan hub.

In summary, Bowden and Payne (2008) conclude that electricity prices exhibit time-varying volatility across each of the MISO hubs. Furthermore, electricity prices exhibit seasonal and time varying volatility due to the non-storability of electricity, inelastic demand and supply, convex marginal costs and potential for market power exerted by generators. Past shocks to the variance are asymmetric and exhibit inverse leverage effects with respect to time-varying volatility. Positive shocks to electricity price increase volatility more than negative shocks of equal magnitude. Lastly, incorporating GARCH models in the ARIMA-framework improves forecasting performance out-of-sample, except for the Michigan hub.

3 Data

This section presents the dataset used in the dissertation, descriptive statistics for the system price, other variables including results from the data preparation procedure.

3.1 The Dataset

The dataset consists of data described in Table 17, collected from NVE[3], The Norwegian Meteorological Institute, and Nord Pool. Data is collected from week 1, 2008 through week 52, 2021, either reported in, or aggregated to weekly frequency. System price is reported in €/MWh, rainfall is collected in millimeters and temperature in Celsius. Rainfall has been aggregated from daily sums to a weekly sum, while temperature has been aggregated from daily averages to a weekly average. Rainfall and temperature observations are from Bergen, Kristiansand, Oslo, Stavanger, Tromsø and Trondheim. Wind power production is reported on a national level and are aggregated to weekly levels from daily data, recorded in MWh. Magazine deviation is the deviation from a 20-year magazine filling level average, and the sum of snow, ground and surface water is an accumulated sum which determines influx to water magazines.

3.2 Variables in Dataset

`price` and `lnprice`

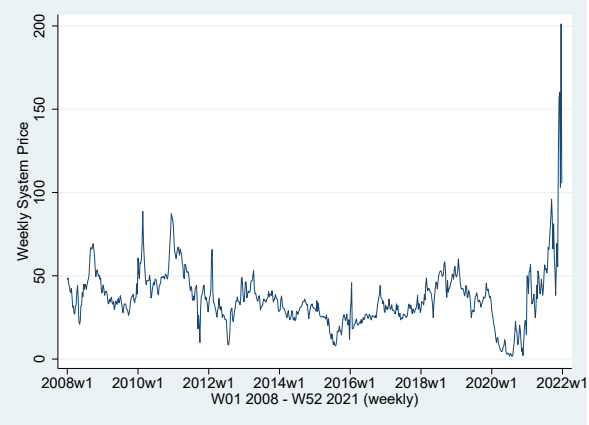

Figure 1: Weekly system price from 01.01.2008 - 31.12.2021.

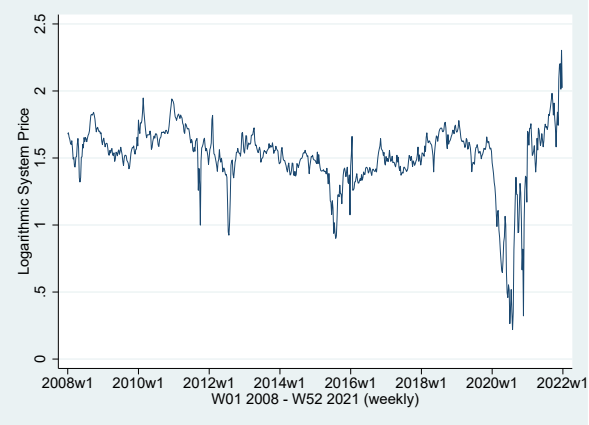

Figure 2: Weekly system price, logarithmic, from 01.01.2008 - 31.12.2021.

The system price for the Nordic market is the theoretical, unconstrained market clearing price for the Nordic region in which most standard contracts considering electricity are

[3]Norwegian Water Resources and Energy Directorate

traded. Calculations are based on aggregated and anonymized orderbooks (OBK) for the Nordic bidding zones, including hourly values of import and export flows of electricity to and from areas neighboring the Nordic bidding zones. *Internal* transmission capacities between Nordic bidding zones are set to infinity, simulating a theoretical situation with unlimited transmission capacity within the Nordic grid system. Considering data demanded by ARCH and GARCH models, the system price is used for simplicity and additional historical data availability (NordPool, 2022, 2020).

The system price is taken from Nord Pool with a weekly frequency. Descriptive statistics for `price` and a logarithmic transformation of the system price, `lnprice`, can be observed in Table 1. System prices are reported from 01.01.2008 to 31.01.2021 in €/MWh and includes 728 observations. Over the period, the lowest recorded system price was 1.6600 €/MWh, while the highest system price recorded was 201.1900 €/MWh. Mean system price across the period was 36.6318 €/MWh, while the standard deviation was 17.7646 €/MWh. Extreme price spikes are present, which can be observed in Figure 1, and the standard deviation equal to 48.17% of the mean indicate a highly volatile system price. Price spikes have previously been discussed in the literature review, for instance by Liu and Shi (2013), and is a common trait for electricity prices even with a weekly frequency. To account for the surge in system price in 2021, a logarithmic transformation is applied which ensures stationarity and contributes to a simplified interpretation, observe Figure 2 compared to Figure 1.

Variable	Sum	Mean	SD	Min	Max	N	Skewness
price	26667.9500	36.6318	17.7646	1.6600	201.1900	728	2.4776
lnprice	1098.45	1.50886	0.2474	0.2201	2.3036	728	-1.8290

Table 1: Descriptive statistics for variables `price` and `lnprice`.

Figure 3 illustrates the system price, including a normal frequency curve, whereas Figure 4 displays the logarithmic transformation of the system price including a normal frequency curve. From Figure 3, distribution plots indicate a right-skewed distribution and Table 1 reveals a right-skewed distribution with a skewness of 2.4776 for the system price. This is consistent with other research by Liu and Shi (2013) and Cifter (2013). The logarithmic

transformation leads to less density around the mean, observed from Figure 4. Furthermore, the distribution appears slightly left-skewed. Skewness equal -1.82900 from Table 1, closer to a normal distribution. Nevertheless, the system price is determined to have a fat tail and excess peakedness at the mean exhibiting leptokurtic behaviour (Brooks, 2019).

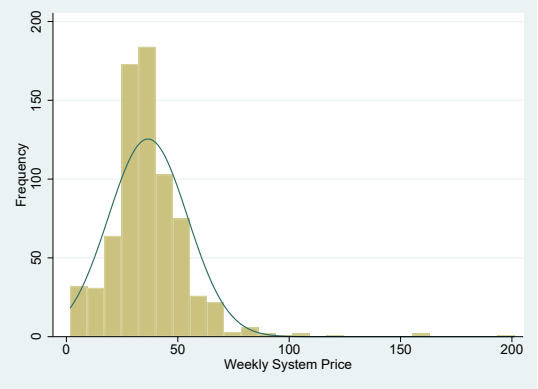

Figure 3: Weekly system price distribution w/ normal frequency curve.

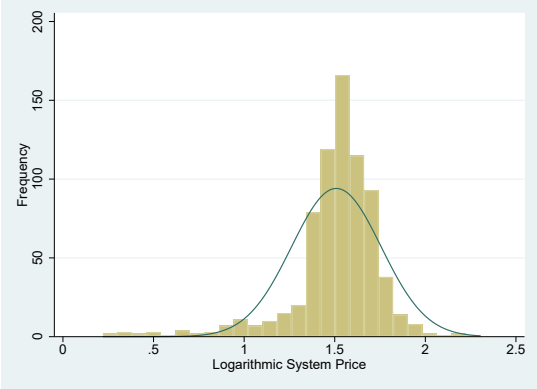

Figure 4: Weekly logarithmic system price distribution w/ normal frequency curve.

`S Adj. Rain` and `S. Adj. Temp.` - Weather Variables

Seasonally adjusted and population weighted temperatures and rainfall for 6 Norwegian cities are included. These cities include Oslo, Bergen, Trondheim, Stavanger, Kristiansand and Tromsø. Variable description can be found in Table 17, and relevant descriptive statistics can be found in Tables 18 and 20 reported in millimeter or degree Celsius, millimeter or degree Celsius deviation from equal week last year depending on the seasonal adjustment, and millimeters or degree Celsius, weighted by population.

Weather variables exhibit strong seasonal patterns, and several methods have been proposed to adjust for this seasonality. This include seasonal dummies, filters or differencing with varying success (Bordignon et al., 2007). Both temperature and rain have been seasonally differenced against equal week the prior year to ensure stationarity[4]. The finalized model framework utilizes population weights based on cities in the dataset, and an extensive reasoning and population weight determination can be found in Section 5.1.2 with population weight formulas in Appendix B.1. Observe Figures 5 and 6 for temperature without seasonal adjustment and seasonally adjusted temperature.

[4]52nd difference taken. $\Delta y_{it} = y_{it} - y_{it-52}$

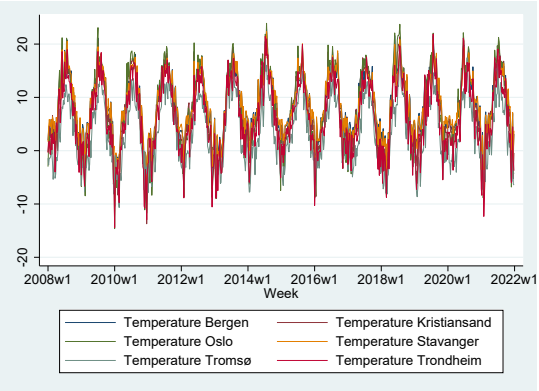

Figure 5: Temperature without seasonal adjustment.

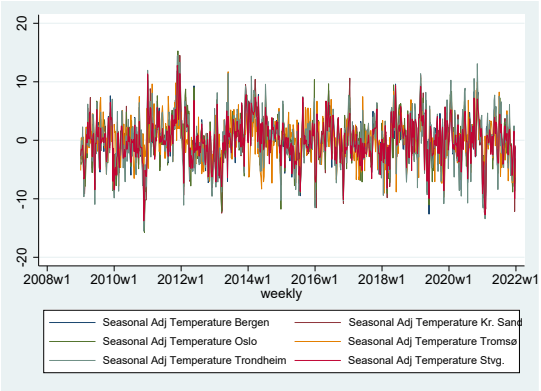

Figure 6: Seasonally adjusted temperature.

`Sum Sno., Gro., Sur. wtr.` and `Sum Magazine Deviation`

Sum of snow, ground and surface water, and sum magazine deviation from NVE are included in the dataset with 728 observations from week 1, 2008 through week 52, 2021, based on data used in calculation of the HBV-model from NVE (Holmqvist, 2013). The data are national sums and can be observed in Table 18. Sum of snow, ground and surface water are utilized in the dissertation to capture inflow to water magazines, regardless of season. Sum of water magazine deviation is taken from a 20-year average and is utilized to capture national direct magazine influx effects and magazine filling level deviation effects.

`Logarithmic Wind Prod.`

Weekly logarithmic and seasonally adjusted wind power production in MWh for Norway is included with summary statistics in appendix, Table 18. Inclusion allows for analyzing the effect wind has on the system price, and therefore encapsulate additional weather effects.

3.3 Data Preparation

Before the analysis, the data has been prepared for time series estimation. Most importantly, unit root process tests have been performed with a DF-GLS unit root process test with 3 lags, and a Philips-Perron unit root process test. The Philips-Perron test has the following specification:

H0: Unit root process.
HA: Stationary process.

The Philips-Perron test performs a similar test as the augmented Dickey-Fuller test, but allows for autocorrelated residuals.

The DF-GLS test test for a unit root process through a GLS regression, which has shown greater performance than the ADF test. The DF-GLS test has the following specification:

H0: Random walk, possibly with drift.
HA: Stationary process around a linear trend.

We reject a unit root process in all variables in contradiction to Koopman et al. (2007). Philips-Perron and DF-GLS test results can be observed in Tables 21 and 22 (Brooks, 2019; Elliott et al., 1996).

4 Empirical Methodology

This section presents the empirical methodology used in the dissertation. ARMA and ARIMA models are presented, including ARCH and GARCH models. Model selection criteria, maximum likelihood estimation and forecasting evalaution measures are explained.

4.1 ARMA and ARIMA Models

Autoregressive Moving Average (ARMA) models are combinations of autoregressive (AR) processes of order p, and moving average processes of order q, resulting in an ARMA(p,q) model. An ARMA(p,q) model describes that some series depends linearly on its own previous values, plus a combination of current and previous values of a white noise error term.

Formally, an ARMA(p,q) model could be written as in Equation (4.1) (Brooks, 2019).

$$\begin{gathered}\phi(L)y_t = \mu + \theta(L)u_t \\ \phi(L) = 1 - \phi_1 L - \phi_2 L^2 - ... - \phi_p L^p \\ \theta(L) = 1 + \theta_1 L + \theta_2 L^2 + ... + \theta_q L^q \\ \text{Another way to specify an ARMA(p,q) follows below:} \\ y_t = \alpha_0 + \sum_{i=1}^{p} \rho_i y_{t-i} + \sum_{i=0}^{q} \theta a_i u_{t-i} \\ E(u_t) = 0; E(u_t^2) = \sigma^2; E(u_t u_s) = 0, t \neq s\end{gathered} \tag{4.1}$$

The ARMA(p,q) model has a geometrically decaying autocorrelation function (ACF) and partial autocorrelation function (PACF). The autocorrelation function describes combinations of behaviour from the AR and MA processes, with AR dominating in the long run, for lags beyond q. The extension from an ARMA(p,q) to an ARIMA(p,d,q) model relies on the characteristic roots in Equation (4.1). If 1 or more characteristic roots of Equation (4.1) is greater than, or equal to 1, the y_t process is integrated of order d, and thus an ARIMA model. The I-term in the ARIMA model therefore indicates the number of differences taken (Enders, 2014).

4.2 ARCH(p) and GARCH (p,q) Models

When analyzing electricity prices, volatility clustering including high, and low-volatility periods are often observed, for example in Figure 1. Therefore, the CLRM assumption of constant error variance[5], homoskedasticity, falls short. Furthermore, electricity prices exhibit volatility clustering where volatility occurs in bursts which can be observed in Figure 7. ARCH and GARCH can be used to model this behaviour, and an ARCH(1) model is described in Equation (4.2).

$$\begin{gathered}y_t = \beta_1 + \beta_2 x_{2t} + \beta_3 x_{3t} + \beta_4 x_{4t} + u_t \\ \sigma_t^2 = \alpha_0 + \alpha_1 u_{t-1}^2 \\ u_t \sim N(0, \sigma_t^2)\end{gathered} \tag{4.2}$$

[5]CLRM = classical normal linear regression model. $u_t \sim N(0, \sigma^2)$ (Brooks, 2019).

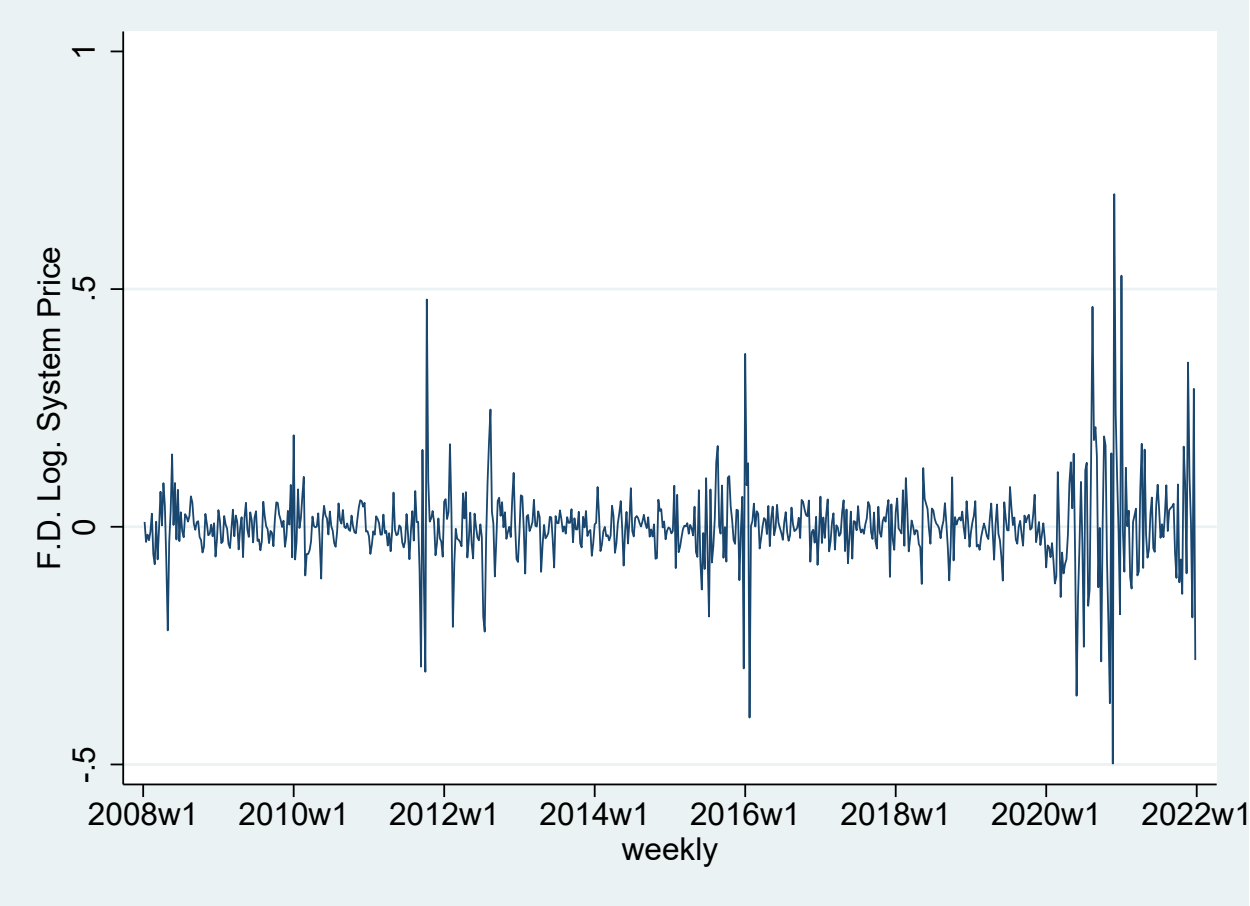

Figure 7: First differenced logarithmic system price from week 1, 2008 through week 52, 2021.

σ_t^2 is the conditional variance and must be strictly positive. However, the ARCH model in Equation (4.2), and other ARCH variants contain limitations which results in less practicality. Therefore, generalized ARCH models (GARCH) are more widely used. Originally developed by Bollerslev in 1986, the GARCH model allows for the conditional variance to be dependent upon previous own lags, is more parsimonious, avoids overfitting, and is less likely to violate non-negativity constraints. A general GARCH(p,q) model is described in Equation (4.3) (Bollerslev, 1986; Brooks, 2019).

$$\sigma_t^2 = \alpha_0 + \sum_{i=1}^{q} \alpha_i u_{t-i}^2 + \sum_{j=1}^{p} \gamma_j \sigma_{t-j}^2 \tag{4.3}$$

In Equation (4.3), the conditional variance depends on q lags of the squared error, and p lags of the conditional variance. It can also be shown that the conditional variance of the error is an ARMA process given by the expression in Equation (4.3) since the conditional variance of u_t is given by $E_{t-1}u_t^2 = \sigma_t^2$. The disturbances of the dependent y_t variable acts

like an ARMA process, which allows for detecting the order for a possible GARCH process in the squared residuals. Furthermore, the GARCH model allows for both autoregressive- and moving average components in the heteroskedastic variance (Enders, 2014).

4.3 Model Selection and Information Criteria

Apart from comparing LLF values, 2 main model selection criteria are used in this paper. 2 of the most popular selection criteria are Akaikes Information Criterion (AIC) and Schwartz Bayesion Criterion (SBC, SBIC or BIC). Inherently, both criteria are a function of the residual sum of squares (RSS) and a penalty for the loss of degrees of freedom from adding extra parameters to the model, see Equation (4.4). Befittingly for model comparison and selection, the value of the information criteria will only be reduced if the RSS outweighs the increased value of the penalty applied. Consequently, AIC and BIC are therefore more widely applied in time series modeling as opposed to R-squared or adjusted R-squared. The penalty term within the AIC is less strict than the penalty term in BIC and it is therefore useful to report both information criteria. In larger sample sizes, BIC has shown to be superior and asymptotically consistent, while AIC will be more biased towards an overparametrized model. On the other hand, AIC may be superior in smaller samples (Enders, 2014). This entails that BIC is strongly consistent, but inefficient, while AIC is inconsistent, but generally more efficient (Brooks, 2019). This emphasizes the aforementioned argument that both criteria, including LLF values should be reported when comparing and selecting models. Consequentially, both AIC and BIC can be negative and lower values are preferred. Since Stata 17 has been used as the main statistical software, Stata 17's formulas are reported in Equation (4.4) (Stata, 2022).

$$
\begin{aligned}
AIC &= -2lnL + 2k \\
BIC &= -2lnL + klnN \\
L &= \textit{Maximized log-likelihood of the model} \\
k &= \textit{Parameters estimated} \\
N &= \textit{Sample size}
\end{aligned}
\tag{4.4}
$$

4.4 Maximum Likelihood Estimation

Maximum Likelihood Estimation (ML) is a common estimation method in econometrics, ensuring both consistency and asymptotically normal distributions. Formally, a set of parameters that are most likely to have produced the observed data values are chosen through construction of a log-likelihood function (LLF) (Brooks, 2019; Pan and Fang, 2002). The LLF is then maximized to find the values of the parameters that maximize the LLF. This method can be used for both linear and non-linear models. For simplicity, calculations are here limited. The general method described is taken from Brooks (2019) and Enders (2014). Derivations can be found in Brooks (2019), appendix 9.1 page 565 and Enders (2014) page 152-154.

In Equation (4.5), $\beta_1, \beta_2, \sigma^2$ are to be estimated, such that an f-function $f(\cdot)$ can be written as the likelihood function $LF(\beta_1, \beta_2, \sigma^2)$.

$$LF(\beta_1, \beta_2, \sigma^2) = \frac{1}{\sigma^T(\sqrt{2\pi})^T} exp\{-\frac{1}{2}\sum_{t=1}^{T}\frac{(y_t - \beta_1 - \beta_2 x_t)^2}{\sigma^2}\} \tag{4.5}$$

The parameter values, $\beta_1, \beta_2, \sigma^2$, that maximizes the function in Equation (4.5) are chosen. Since this equation is difficult to differentiate due to the T-term, logarithms of the probability density function, Equation (4.6), is taken and then differentiated, assuming the y's are i.i.d.[6].

$$\begin{aligned} &f(y_1, y_2, ..., y_T|\beta_1 + \beta_2 x_1, \beta_1 + \beta_2 x_2, ..., \beta_1 + \beta_2 x_T, \sigma^2) \\ &= \prod_{t=1}^{T} f(y_t|\beta_1 + \beta_2 x_t, \sigma^2) \text{ for } t = 1, ..., T \end{aligned} \tag{4.6}$$

Through transformation this results in the log-likelihood function (LLF), Equation (4.7).

$$LLF = -\frac{T}{2}ln\sigma^2 - \frac{T}{2}ln(2\pi) - \frac{1}{2}\sum_{t=1}^{T}\frac{(y_t - \beta_1 - \beta_2 x_t)^2}{\sigma^2} \tag{4.7}$$

[6] i.i.d. = independent and identically distributed random variables.

By differentiating Equation (4.7) w.r.t $\beta_1, \beta_2, \sigma^2$, and then minimizing by equaling to zero, the maximum likelihood estimators (denoted by hats) are obtained in Equation (4.8).

$$\begin{aligned} \sum (y_t - \hat{\beta}_1 - \hat{\beta}_2 x_t) &= 0 \\ \sum y_t - \sum \hat{\beta}_1 - \sum \hat{\beta}_2 x_t &= 0 \\ \sum y_t - T\hat{\beta}_1 - \hat{\beta}_2 \sum x_t &= 0 \\ \frac{1}{T} \sum y_t - \hat{\beta}_1 - \hat{\beta}_2 \frac{1}{T} \sum x_t &= 0 \\ \hat{\beta}_1 &= \bar{y} - \hat{\beta}_2 \bar{x} \end{aligned} \tag{4.8}$$

We can also utilize first derivatives to obtain estimators for $\hat{\beta}_2$ in Equation (4.9).

$$\hat{\beta}_2 = \frac{\sum y_t x_t - T\bar{x}\bar{y}}{(\sum x_t^2 - T\bar{x}^2)} \tag{4.9}$$

Observe that Equations (4.8) and (4.9) are equal to OLS estimates of the intercept and slope coefficients. However, an estimate of $\hat{\sigma}^2$ can be obtained which equals the result in Equation (4.10).

$$\hat{\sigma}^2 = \frac{1}{T} \sum \hat{u}_t^2 \tag{4.10}$$

The estimator in Equation (4.10) for the error variance is biased, albeit consistent[7].

4.5 Volatility and Model Evaluation

4.5.1 Volatility Measures

The dissertation employs a realized volatility measure with inspiration from Day and Lewis (1992) and Simonsen (2005). Formulae are set out in Equation (4.11). Observe that historical volatility mainly used by Day and Lewis (1992), $\sigma(t,T)$ is approximately equal to squared returns for the dataset, similar to results from Simonsen (2005). Realized variance - `rvar` as calculated in Equation (4.11) is applied (Brooks, 2019).

$$\begin{aligned} lnreturn(t) &= ln(\frac{price + \Delta price}{price}) \text{ — Logarithmic return} \\ \sigma(t,T) = rvar &= (lnreturn(t) - \mu)^2 \approx lnreturn(t)^2 \text{ — Realized variance} \end{aligned} \tag{4.11}$$

[7] As $T \to \infty, T - k \approx T$

4.5.2 Model Evaluation

When comparing time series models, several methods can be applied. The methods described here are from Brooks (2019) and Enders (2014) and include RMSE, MAE, MAPE and Theil's U.

$$RMSE = \sqrt{\frac{1}{T-(T_1-1)}\sum_{t=T_1}^{T}(y_{t+s}-f_{t,s})^2} \tag{4.12}$$

Where T = total sample size, T_1 = first out of sample forecast observation. RMSE is the root mean square error and defines the standard deviation of the residuals and can be interpreted in terms of measurement units.

$$MAE = \frac{1}{T-(T_1-1)}\sum_{t=T_1}^{T}|y_{t+s}-f_{t,s}| \tag{4.13}$$

MAE is the mean absolute error and the average absolute forecast error.

$$MAPE = \frac{100}{T-(T_1-1)}\sum_{t=T_1}^{T}|\frac{y_{t+s}-f_{t,s}}{y_{t+s}}| \tag{4.14}$$

MAPE is the mean absolute percentage error, and thus the MAE in percentages.

$$U = \frac{\sqrt{\sum_{t=T_1}^{T}(\frac{y_{t+s}-f_{t,s}}{y_{t+s}})^2}}{\sqrt{\sum_{t=T_1}^{T}(\frac{y_{t+s}-fb_{t,s}}{y_{t+s}})^2}} \tag{4.15}$$

Where $fb_{t,s}$ is a forecast from a benchmark model. Theil's U-statistic is useful for comparing models where a U-statistic equal to 1 implies equal model accuracy to a naïve forecast. U-statistics below 1 implies a superior forecast model, and vice versa for U-statistics larger than 1.

5 Results

The section presents results from ARIMA and ARIMA-GARCH estimation. ARIMA specification and population weight determination are first presented before assessing model fit and in-sample properties. Additionally, a variety of ARIMA-GARCH models are estimated to study system price, volatility and in-sample fit before results are discussed.

5.1 ARIMA Specification and Population Weight Determination

In this section an ARIMA(p,d,q) model is specified through the 3-step Box-Jenkins approach. Next, population weights for seasonally adjusted temperature and rainfall are determined through an ARIMA specification. Finally, the analysis is extended by analyzing autocorrelation functions for the residuals and testing for ARCH and GARCH effects with Engle and Lagrange's multiplier test.

5.1.1 ARIMA Specification

The autoregressive integrated moving average, ARIMA(p,d,q) specification has been chosen due to flexibility. Inclusion of both autoregressive processes of order p, moving average processes of order d, and integrated processes of order d allows for a flexible estimation procedure and is therefore a desirable initial model framework.

Initially, an ARIMA(0,0,0) model with population weights based on cities in the dataset is estimated through log-likelihood maximization in STATA. The reasoning for choosing appropriate population weights are further elaborated on in Section 5.1.2. ACF and PACF plots of residuals can be observed in Figures 8 and 9 where the series displays an AR1 signature with a gradually decaying ACF and a PACF with a sharp cutoff at lag 1 (Nau, 2020). An AR(1) term is therefore included, and an ARIMA(1,0,0) model[8] is further estimated with ACF and PACF plots in Figures 10 and 11 and model in Equation (A.0).

$$lnprice_t = \alpha_0 + \beta' \mathbf{X}_t + \rho lnprice_{t-1} + error_t \tag{A.0}$$

$\mathbf{X}$ is a vector of the regressors in Table 17, except lnprice and rvar.

[8]This is equivalent to an AR(1) model.

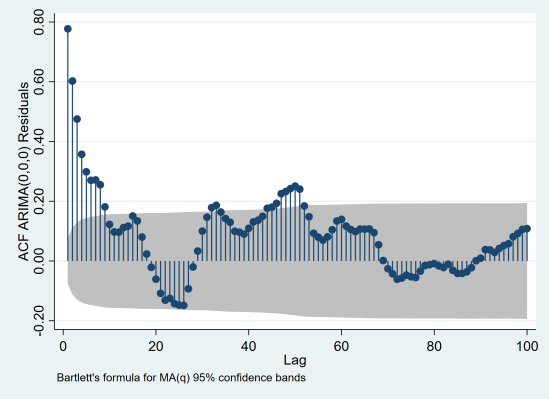

Figure 8: ACF for ARIMA(0,0,0)

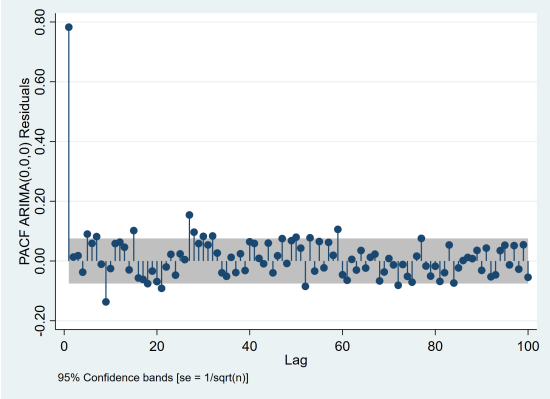

Figure 9: PACF for ARIMA(0,0,0)

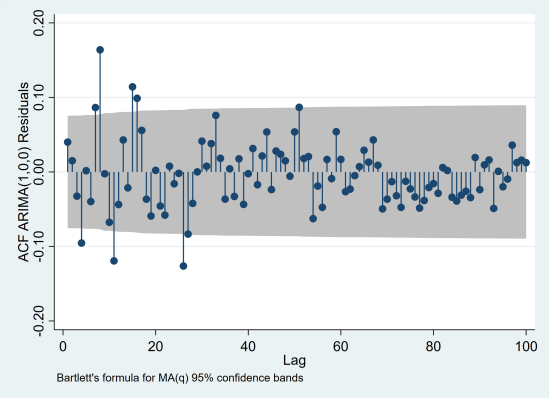

Figure 10: ACF for ARIMA(1,0,0)

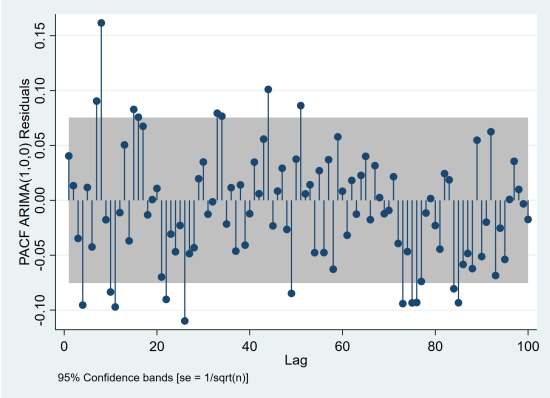

Figure 11: PACF for ARIMA(1,0,0)

Analyzing ACF and PACF plots for the ARIMA(1,0,0) model in Figures 10 and 11, both the ACF and PACF are switching signs throughout the lags. However, the standard deviation of the residuals has decreased from the ARIMA(0,0,0), observe Table 3, and the ACF and PACF are converging towards 0. The ARIMA(1,0,0) is therefore preferred over the ARIMA(0,0,0). ACF and PACF plots from in Figures 10 and 11 does however indicate a possibility for improvement. The dissertation proceeds with the Box-Jenkins 3-step approach as described in Brooks (2019):

1. Identification. ACF and PACF plots are used to determine the model order.
2. Estimation. Log-likelihood maximization in Stata 17 is applied.
3. Diagnostics checking. Residual diagnostics and Ljung-Box Q tests is applied.

Inspecting the PACF plot for the ARIMA(1,0,0) model, evidence of slight underdifferencing

is present with 2/20 first lags outside of the 95% confidence band. Several other lags are outside of the 95% confidence bands for longer lag-lengths. Due to parsimony, only PACF values above 0.1 are included, AR lags 8 and 26. A similar procedure is adopted when inspecting ACF, including MA lags 8, 11, 15 and 26 in the ARIMA model.

Therefore, an ARIMA model containing AR lags 1, 8 and 26 and MA lags 8, 11, 15 and 26 is estimated with log-likelihood maximization in Stata. Afterwards, statistically insignificant AR and MA-terms are removed and a Ljung-Box-Q statistic for autocorrelated residuals is calculated for all models. The appropriate model is selected based on the criteria, including AIC, BIC and further residual analysis. Model results can be observed in Table 12 as model 1, estimated ARIMA model in Equation (A.1), and information criteria in Table 4.

$$lnprice_t = \alpha_0 + \beta' \mathbf{X}_t + \rho_1 lnprice_{t-1} + \rho_2 lnprice_{t-8} + \rho_3 lnprice_{t-26}$$
$$+\theta_1 u_{t-8} + \theta_2 u_{t-11} + \theta_3 u_{t-15} + \theta_4 u_{t-26} + error_t \qquad \text{(A.1)}$$

$\mathbf{X}$ is a vector of the regressors in Table 17, except lnprice and rvar.

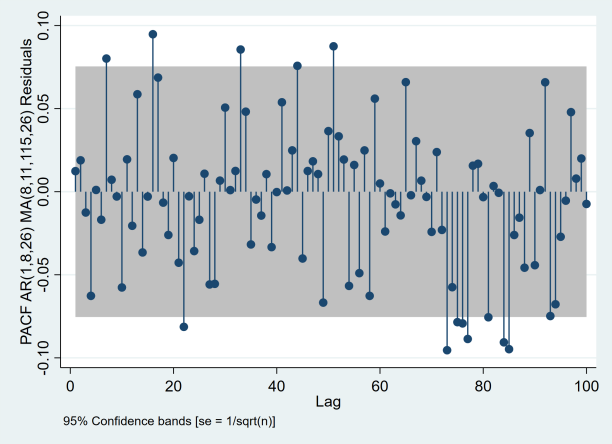

Figure 12: PACF AR(1,8,26) MA(8,11,15,26)

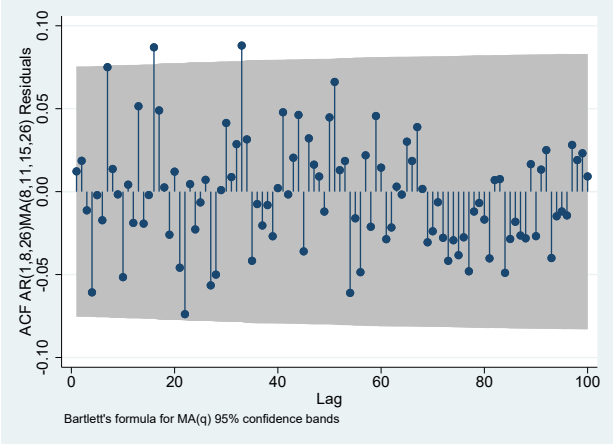

Figure 13: ACF AR(1,8,26) MA(8,11,15,26)

The estimated ARIMA model results in a statistically significant AR-1 lag on all relevant significance levels and a highly autoregressive process of order 1 equal to 0.8795, including statistically significant moving average lags. AR-lags 8 and 26 are statistically insignificant on all relevant significance levels with coefficients equal to -0.0095 and 0.0003. A Ljung-Box-Q statistic results in a p-value equal to 0.552, an no rejection of the null hypothesis of a

white noise process within the residuals at a 52.2% significance level. Ljung-Box-Q statistics can be found in Table 2. From Table 4, AIC and BIC are -1659.4367 and -1546.5319, an improvement from the less complex ARIMA models. The model is marked as number 1 in Table 12.

Based on results above, the 26th AR-lag is removed from the model. The model equation can be found in Equation (A.2), an ARIMA model with AR-lags 1 and 8, and MA-lags 8, 11, 15, and 26. AR-lag 1 is statistically significant on all relevant significance levels with coefficient equal to model 1, 0.8795. All MA-terms are still statistically significant on a 5% level. AR-lag 8 is still statistically insignificant on a 60.8% significance level. Ljung-Box-Q statistic results in a Q-stat equal 38.8209 and a p-value equal 0.5233, rejection of the null hypothesis on a 52.33% significance level, and therefore similar results to model 1. From Table 12, AIC and BIC are more negative, implying an improved model specification. The model is marked as 2 in Table 12 and Ljung-Box-Q statistics can be found in Table 2.

$$\begin{aligned} lnprice_t = \alpha_0 + \beta' \mathbf{X}_t + \rho_1 lnprice_{t-1} + \rho_2 lnprice_{t-8} \\ + \theta_1 u_{t-8} + \theta_2 u_{t-11} + \theta_3 u_{t-15} + \theta_4 u_{t-26} + error_t \end{aligned} \tag{A.2}$$

X is a vector of the regressors in Table 17, except lnprice and rvar.

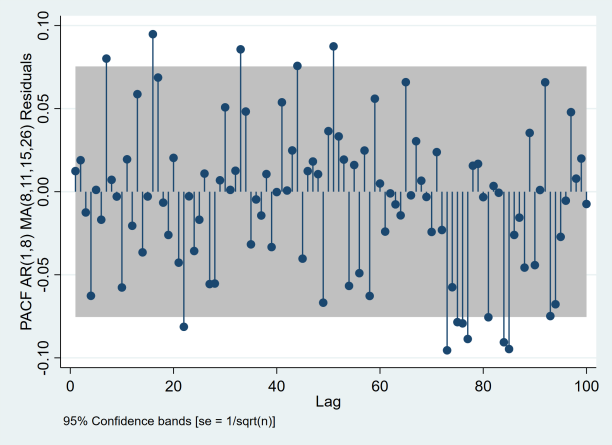

Figure 14: PACF AR(1,8) MA(8,11,15,26)

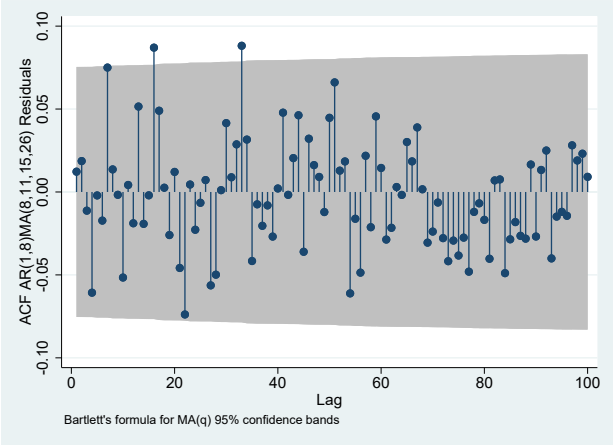

Figure 15: ACF AR(1,8) MA(8,11,15,26)

Next, the 8th AR-lag is removed from the model due to statistical insignificance and an ARIMA model with AR-lag 1 and MA-lags 8, 11, 15, and 26 is estimated, marked as model

3 in Table 12 is estimated, with model in Equation (A.3). The AR-1 lag and the 4 MA-lags 8, 11, 15, 26 are statistically significant on a 5% significance level. Completed Ljung-Box Q-statistic results in a Q-statistic equal to 38.263 and a p-value equal to 0.5276 and continued rejection of the null hypothesis, now on a 52.75% significance level. From Table 12, AIC and BIC are also more negative, indicating an improved model specification over previously estimated models. Ljung-Box-Q statistics can be found in Table 2.

$$lnprice_t = \alpha_0 + \beta' \mathbf{X}_t + \rho_1 lnprice_{t-1}$$
$$+\theta_1 u_{t-8} + \theta_2 u_{t-11} + \theta_3 u_{t-15} + \theta_4 u_{t-26} + error_t \quad \text{(A.3)}$$

$\mathbf{X}$ is a vector of the regressors in Table 17, except lnprice and rvar.

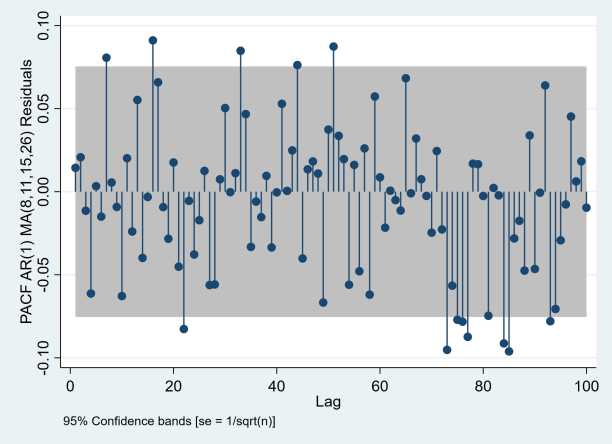

Figure 16: PACF AR(1) MA(8,11,15,26)

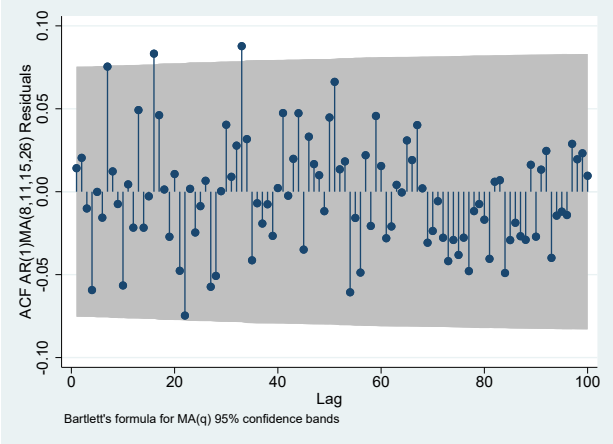

Figure 17: ACF AR(1) MA(8,11,15,26)

Furthermore, ACF and PACF plots from model 1-3 in Figures 12, 14 and 16 are inspected. A generally tighter ACF and PACF plot can be observed, indicating a notable improvement from the ARIMA(1,0,0). No ACF or PACF values surpasses 0.10, with fewer values exceeding the 95% confidence band for the more complex ARIMA variants. General convergence within ACF and PACF towards 0 is observed. Residual mean and standard deviation for several ARIMA-models can be observed in Table 3, where the more complex ARIMA variants results in lower residual standard deviation which further emphasizes that a more complex ARIMA model is appropriate for the data. Observe from Table 12 that several coefficients are statistically insignificant, where some variables produce awkward and debatable results.

Model	DF	P-value	Q-stat
AR(1,8,26)MA(8,11,15,26))	40	0.5228	38.8300
AR(1,8)MA(8,11,15,26)	40	0.5233	38.8209
AR(1)MA(8,11,15,26)	40	0.5276	38.7263

Table 2: Portmanteu (Ljung-Box)-Q test.

All 3 models report the effect of temperature deviation in Trondheim and rainfall deviation in Bergen, Kr. Sand and Tromsø on the system price as statistically significant on a 10% significance level. However, 1 mm. additional rainfall against equal week last year in Kr. Sand, Stavanger or Trondheim is expected to reduce the system price by $\approx 252\%$, $\approx 46.71\%$ or $\approx 44.20\%$ respectively, debatable results. Rainfall deviation in Bergen has an estimated negative effect of $\approx$ -22% on the system price by 1 mm. more rainfall deviation. Estimated temperature effects on system price are generally small, with the largest effect in Oslo and Kr. Sand with 2.06% and 1.77%, both positive. All other temperature estimates are below 1%, regardless of sign. Therefore, conclusions regarding expectation, supply, consumption and demand based effects alongside temperature and rainfall cannot be drawn. The AR-1 coefficient is still statistically significant on all relevant significance levels and reveals a highly autoregressive process of order one, ≈ 0.88. The ARIMA model with AR-lag 1 and MA-lags 8, 11, 15 and 26 is deemed superior against the other ARIMA alternatives based on residual statistics and ACF and PACF.

5.1.2 Population Weight Determination

As previously described, a population weight determination process has been applied to select appropriate population weights for temperature and rainfall. The process is a 3-step procedure described below.

1. Appropriate population weight is chosen.
2. Each city is assigned a population weight on rainfall and temperature based on population in the city.
3. The result is population weighted rainfall and population weighted temperature.

Variable	Mean	Std. Dev
ARIMA(0,0,0) Residual	2.16e-10	0.1358477
ARIMA(1,0,0) Residual	-0.0001488	0.0714143
ARIMA(2,0,0) Residual	-0.0001303	0.0713314
ARIMA(3,0,0) Residual	-0.0001238	0.0713241
ARIMA(0,1,0) Residual	1.42e-10	0.0733939
ARIMA(0,2,0) Residual	3.16e-10	0.1032708
ARIMA(0,3,0) Residual	1.08e-10	0.1751914
ARIMA(0,0,1) Residual	1.23e-06	0.0952594
ARIMA(0,0,2) Residual	9.14e-06	0.08298262
ARIMA(0,0,3) Residual	9.69e-07	0.0768985
AR(1,8,26)MA(8,11,15,26) Residual	-0.0000983	0.0683259
AR(1,8)MA(8,11,15,26) Residual	-0.0000974	0.0683259
AR(1)MA(8,11,15,26) Residual	-0.0000105	0.0683325

Table 3: Residual sum and standard deviation for ARIMA variants.

- Changes in rainfall deviation are expected to affect the system price.
  Population weighted rainfall capture the effect of rainfall weighted by population in each city. In periods with heavy rainfall, the market may expect a lower system price due to higher expected supply. This effect may vary in size, depending on regional population. When seasonally adjusted, this is therefore both an **expectations and a supply effect with deviations from the same week last year.**

- Changes in temperature deviation are expected to change the system price.
  Population weighted temperature captures the effect of temperature weighted by population in each city. In periods with high temperatures power consumption is lower than average, contributing to less demand for power. This effect may vary in size, depending on regional population. When seasonally adjusted, this is therefore both a **consumption and a demand effect with deviations from the same week last year.**

The appropriate model has been chosen based on statistical significance, omitted variables, information criteria and relevance for the thesis statement.

Model	LL	AIC	BIC
ARIMA(0,0,0)	390.74325	-745.4865	-664.195
ARIMA(1,0,0)	825.6698	-1613.34	-1527.532
ARIMA(2,0,0)	826.4965	-1612.993	-1522.669
ARIMA(3,0,0)	826.5677	-1611.135	-1516.295
ARIMA(0,1,0)	805.759	-1575.518	-1494.253
ARIMA(0,2,0)	574.3857	-1112.771	-1031.533
ARIMA(0,3,0)	2217.8375	-399.6751	-318.4637
ARIMA(0,0,1)	630.6604	-1223.321	-1137.513
ARIMA(0,0,2)	723.9774	-1407.955	-1317.631
ARIMA(0,0,3)	775.5875	-1509.175	-1414.335
AR(1,8,26)MA(8,11,15,26)	854.7183	-1659.4367	-1546.5319
AR(1,8)MA(8,11,15,26)	854.7182	-1661.4365	-1553.0479
AR(1)MA(8,11,15,26)	854.6489	-1663.2977	-1559.4253

Table 4: Information criteria for ARIMA variants.

The ARIMA model with AR-lag 1 and MA-lags 8, 11, 15 and 26 from the previous section is estimated with different weights on rainfall and temperature. 1 model has been estimated without population weights, 1 with the city's population as a proportion of total national population, and 1 model with the city's population as a proportion of total population within the dataset. Formulae can be observed in Equation (`B.1`) with population weights in Tables 15 and 16. Estimation results are reported in Table 11, the model in Equation (`A.3`) for varying temperature and rainfall population weights, and a statistical significance table in Table 5. Observe statistically insignificant and omitted variables due to multicollinearity suggesting in general high correlation between variables.

Variable	Model No Weights	Model Nat. Weights	Model City Weights
S.Adj Temp. Bergen	1%	1%	Insignificant
S.Adj Temp. Kristiansand	Insignificant	Insignificant	Insignificant
S.Adj Temp. Oslo	10%	10%	Insignificant
S.Adj Temp. Tromsø	Insignificant	Omitted	Insignificant
S.Adj Temp. Trondheim	Insignificant	Insignificant	10%
S.Adj Temp. Stavanger	5%	0%	Insignificant
S.Adj Rain Bergen	Omitted	Omitted	10%
S.Adj Rain Kristiansand	Omitted	Omitted	10%
S.Adj Rain Oslo	Omitted	Insignificant	Insignificant
S.Adj Rain Stavanger	Omitted	Omitted	Insignificant
S.Adj Rain Tromsø	Insignificant	Insignificant	10%
S.Adj Rain Trondheim	Insignificant	Insignificant	Insignificant
Log. Wind Production	5%	5%	5%
Sum Magazine Deviation	0%	0%	0%
Sum Sno., Gro., and Sur. wtr	0%	0%	1%
Dummy = 1 for 2020	0%	0%	0%
AR(1)	0%	0%	0%
MA(8)	0%	0%	0%
MA(11)	0%	0%	1%
MA(15)	1%	5%	5%
MA(26)	0%	0%	0%

Table 5: Statistical significance table in % from estimates reported in Table 11.

Estimation results along with AIC, BIC and LL are reported in Table 11. Aforementioned and future ARIMA models are estimated with log-likelihood maximization and population weighted and seasonally adjusted temperature and rain, logarithmic wind power production, magazine deviation, a dummy for 2020, and the sum of snow, ground, and surface water. All 3 models report statistically significant results at a 5% significance level for logarithmic wind

power production, magazine deviation, the dummy variable, and the sum of snow, ground, and surface water. The effects are of similar magnitude in all models. AR and MA-terms are statistically significant in all models.

AIC and BIC favours the estimated ARIMA model without weights, while the log-likelihood (LL) functions favour the model with city weights. Although AIC and BIC favour the model without population weights, 4 variables for rainfall are omitted due to collinearity. Considering the thesis statement, the model without population weights is discarded. When comparing national weights and city weights, AIC favours the former, while BIC favours the latter. Applying equal reasoning as before, and since BIC can be argumented for as superiour in larger samples, see section 4.3, the model with national weights is discarded due to relevance, and the model with city weights is preferred.

5.1.3 Model Fit and In-Sample Properties

Model fit and in-sample properties are considered through a static 1-step forecast and accuracy statistics. The static forecast relies on lagged values of the data from week 1, 2009 until the end of the sample and are reported in Figure 18 for the ARIMA model with AR-lag 1, MA-lags 8, 11, 15 and 26, and population weighted rainfall and temperature by cities. Forecast accuracy statistics, are reported in Table 6. These statistics are more relevant when comparing models against each other, but observe that Theil's U has a value below 1, indicating a better forecast than a naïve forecast. Visually from Figure 18 the model follows the trend of the system price including periods of high volatility during 2020 and 2021.

Measure	N	Value
RMSE	676	0.06828198
MAE	676	0.04310136
MAPE	676	3.608341%
Theil's U	676	0.69897952

Table 6: Forecasting criteria to assess model fit for the preferred ARIMA model.

5.2 Heteroskedasticity

Leptokurtic behaviour, volatility clustering, and leverage effects have previously been found present within electricity price by for instance Liu and Shi (2013); Bowden and Payne (2008) and Koopman et al. (2007). Therefore, ARCH and GARCH models are reasonable candidates to expend the analysis and explicitly model volatility. Several tests can be performed to identify non-linear time series structure including the Ramsey RESET test and the BDS test. However, the most specific method for ARCH and GARCH models are perhaps to study ACF and PACF, including Engle's Lagrange multiplier test for ARCH effects (Brooks, 2019; Enders, 2014).

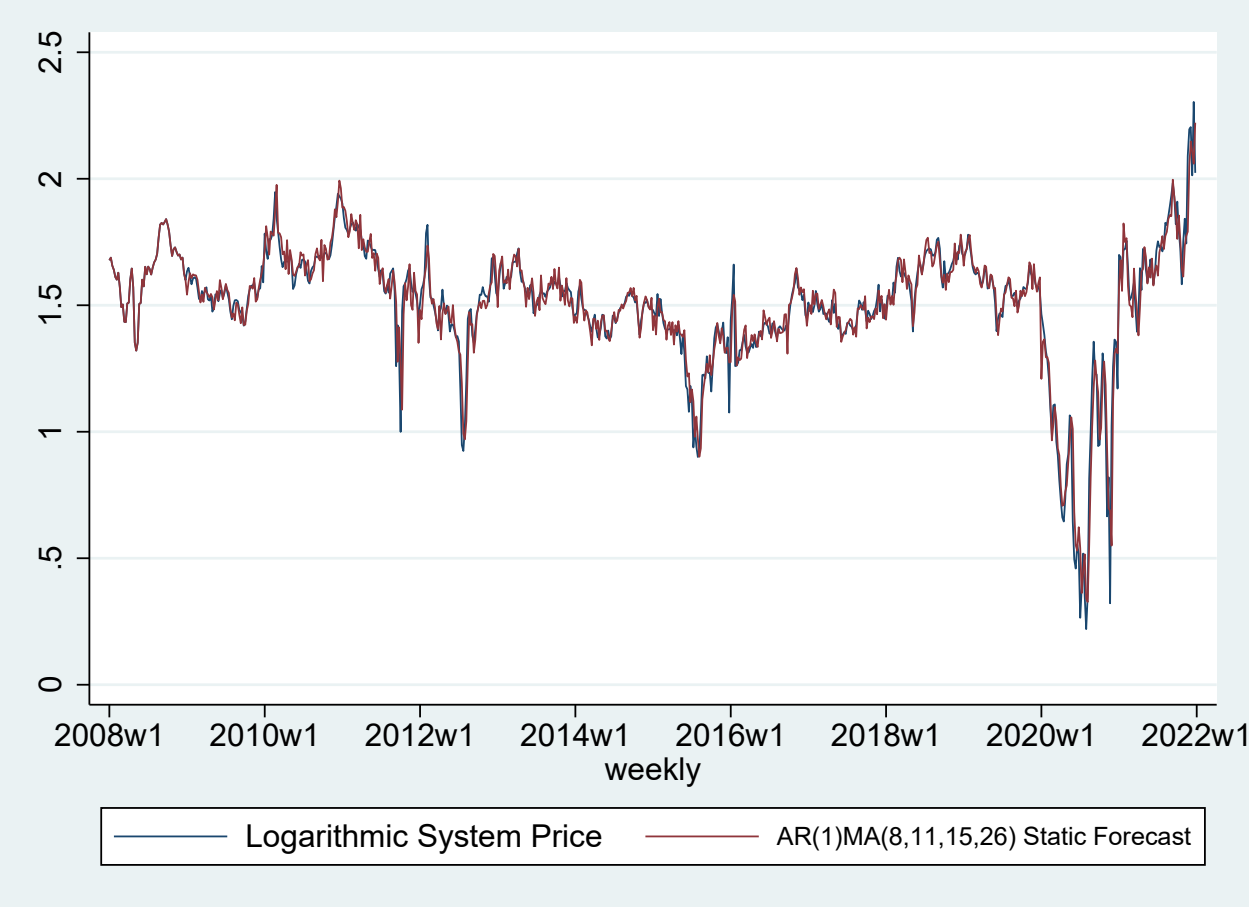

Figure 18: Static in-sample system price forecast for the preferred ARIMA model. Start from week 1, 2009.

Firstly, squared residual ACF and PACF are visually analyzed with additional residual diagnostics in Figure 19. Autocorrelations outside of the 95% confidence bands indicate ARCH effects, which can be observed present in lags 1, 2, 3, 4, 5, 6, 11, 12, 14, 15, 21

and 26. Furthermore, Engle's Lagrange multiplier test for ARCH effects is computed with the process described in Brooks (2019). A linear regression is estimated, squared residuals are saved, and a test statistic $TR^2 \sim \chi^2$ is calculated, where T = number of observations. Results can be observed in Table 7 with evidence of ARCH effects on 26 lags. It is therefore evident the continuation of the dissertation should adopt models that capture ARCH and GARCH effects.

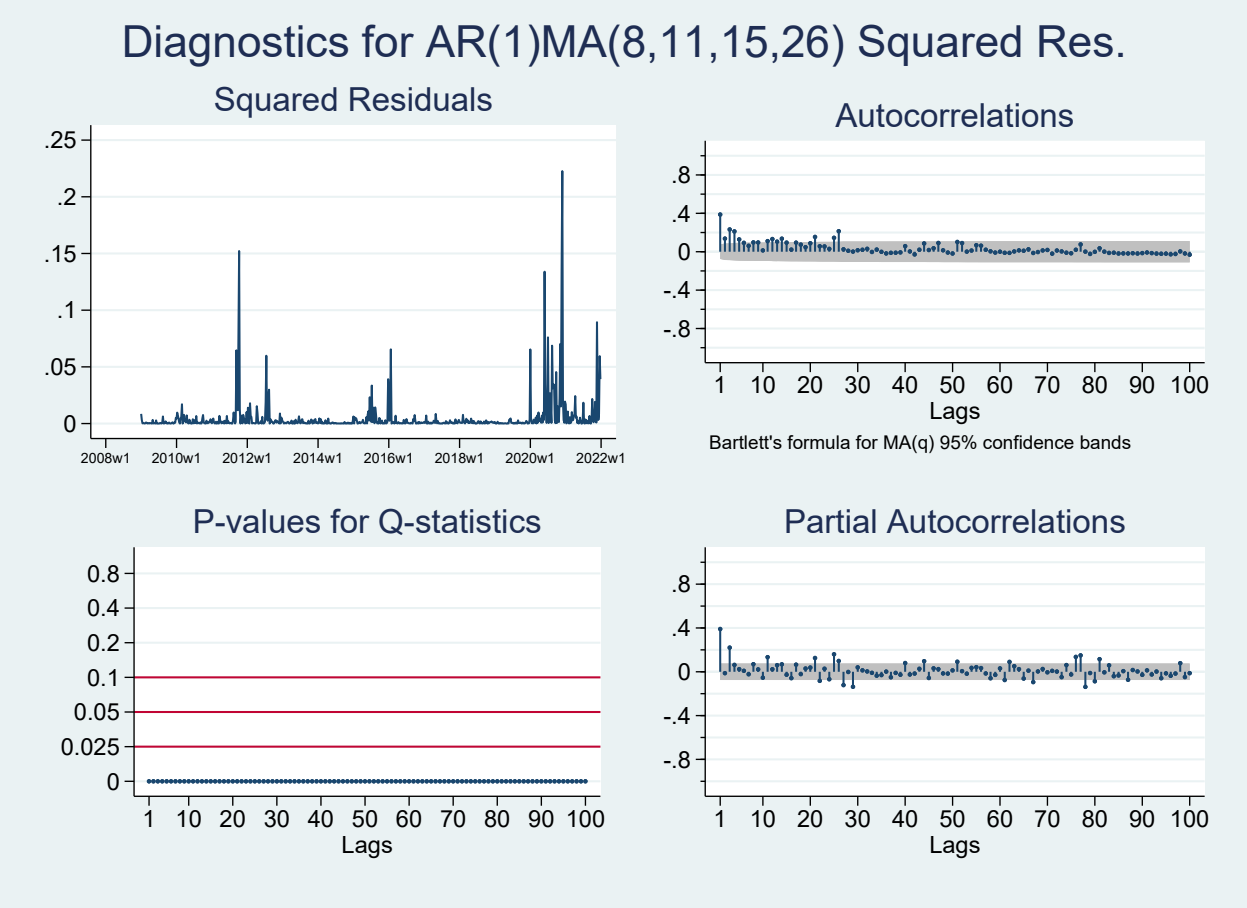

Figure 19: ARCH diagnostics for squared residuals from preferred ARIMA model.

N	χ^2	DF	P	Lags
650	297.944	26	0.0000	26

Table 7: LM test for ARCH effects.

5.3 ARIMA-GARCH Variants

In this section several ARIMA-GARCH models are estimated with different restrictions to mainly study the effect temperature and rainfall has on the system price and volatility, including expectation and supply effects from rainfall, and consumption and demand effects from temperature. Results are comprehensively discussed in Section 5.5. Extensive work to determine an appropriate GARCH specification has previously been done. A particularly thorough article compares 330 ARCH-type models and determines the GARCH(1,1) superior, which is similar to other GARCH-specifications previously discussed by Hansen and Lunde (2005). The GARCH(1,1) model has also been widely applied in financial time series and is therefore chosen as the dissertations initial volatility framework (Brooks, 2019; Enders, 2014). The ARIMA-GARCH models are estimated in Stata 17 with log-likelihood maximization.

5.3.1 ARIMA-GARCH Specification

The previously developed ARIMA model with AR-lag 1 and MA-lags 8, 11, 15 and 26 is declared as the starting point. Initially, a GARCH(1,1) is added to the ARIMA, creating an ARIMA-GARCH model specification estimated with log-likelihood maximization simultaneously. Subsequently, a residual diagnosis check to analyze whether the residuals satisfy the requirements for a Gaussian white noise process is executed, including an assessment of model fit for the system price and volatility. This procedure is similar to Liu and Shi (2013). Estimation results from the ARIMA-GARCH can be observed in Table 13, model 0 with the model in Equation (G.0).

$$
\begin{aligned}
lnprice_t &= \alpha_0 + \beta' \mathbf{X}_t + \rho_1 lnprice_{t-1} \\
&+ \theta_1 u_{t-8} + \theta_2 u_{t-11} + \theta_3 u_{t-15} + \theta_4 u_{t-26} + \varepsilon_t \\
\varepsilon_t &= \sigma_t^2 = \alpha_0 + \alpha_1 u_{t-1}^2 + \gamma_1 \sigma_{t-1}^2
\end{aligned}
\tag{G.0}
$$

$\mathbf{X}$ is a vector of the regressors in Table 17, except lnprice and rvar.

ε_t defines the GARCH(1,1) specification of the ARIMA-GARCH.

Temperature coefficients for all cities are statistically insignificant. The effects are smaller than the ARIMA-estimation, indicating that temperature deviation through consumption

and demand effects have a smaller effect on system price when including time-varying conditional volatility, with estimates below 1% except for Kr. Sand. Estimates for Tromsø have changed signs, from 1.04% to -0.15%.

Rainfall deviation coefficients are smaller against the ARIMA-model for all cities except Trondheim, where 1mm. more rainfall deviation increase the system price by $\approx 60.12\%$, opposed to $\approx 44.20\%$. The large, positive effect indicates an imprecise estimate considering previous evidence. Coefficient for Oslo have switched signs however the effect is small, equal to -1.03%. Rainfall deviation in Bergen is statistically significant on a 1% significance level, reducing system price by -16.6%, ceteris paribus. Empirically the effect is reasonable due to Vestlands significance in hydropower production (Tvede, 2017). The effect is smaller than estimates from ARIMA modeling.

However, several rainfall coefficients are statistically insignificant or produce results that are difficult to interpret. The system price is expected to decrease over $\approx 103\%$ per millimeter increased rainfall deviation in Kristiansand, $\approx 43.8\%$ in Stavanger and $\approx 60.12\%$ in Trondheim. Even though results, except for Trondheim, are smaller than results from ARIMA modeling, the effects rainfall has through expectation, supply and population are implausibly large, considering the complex structure which determines the system price. Other variables such as wind power production, magazine deviation and snow, surface and ground water are statistically significant on a 1% significance level, and reduce the system price accordingly. The effects are empirically intuitive, considering their importance in calculating hydrological balance and magazine filling levels. In summary, there is little evidence that rainfall and temperature in cities through expectation, supply, consumption and demand effects affects system price (NVE, 2020, 2021).

Inclusion of ARCH and GARCH effects reveal a highly volatile system price with statistically significant coefficients on all relevant significance levels. From the ARCH-term for model 0 in Table 8 it can be observed that shocks to volatility today through the ARCH term, α_1, equal ≈ 0.7412. Correlation between the variance over two periods through the GARCH term, γ_1, equal ≈ 0.4043, and evidence of volatility clustering. Summarized, ARCH

and GARCH-terms equal 1.1455 which implies exponential volatility persistence, and non-stationary variance. The ARIMA-GARCH against realized variance can be observed in Figure 20. Periods of high and low volatility are acknowledged, somewhat captured by the model, confirming exponential volatility persistence. Results are similar to estimates from the SGARCH, QGARCH, GJRGARCH and EGARCH models estimated by Liu and Shi (2013). Lastly, AIC and BIC have both vastly improved against the ARIMA-specification, indicating a better model fit.

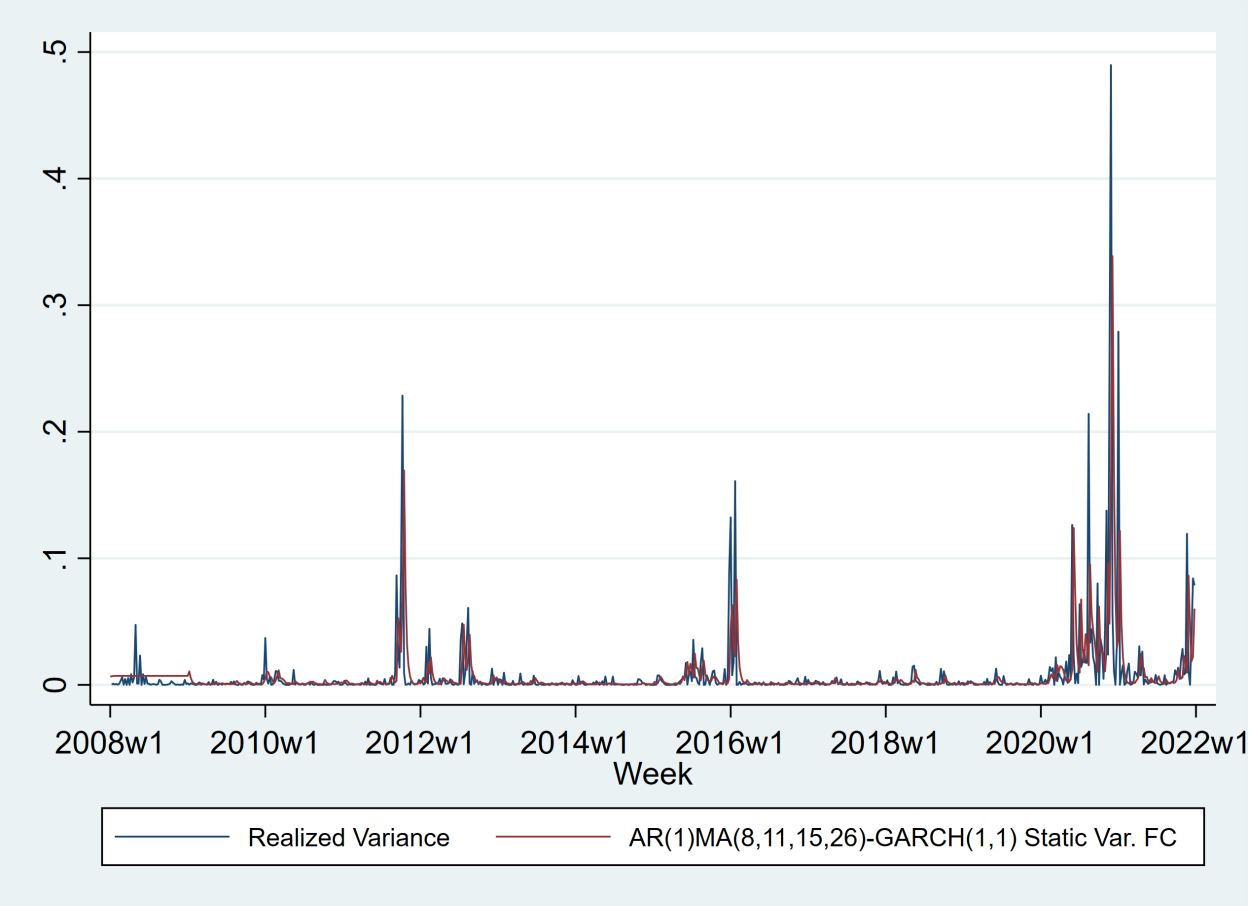

Figure 20: Visual model fit for the AR(1)MA(8,11,15,26)-GARCH(1,1) for conditional volatility against realized variance.

The AR(1) and MA(11,26) terms are statistically significant, whereas MA(8,15) are statistically insignificant. Therefore, MA terms (8,15) are dropped from the model and an ARIMA-GARCH with AR-lag 1, MA-lags 11 and 26 and a GARCH(1,1) is estimated and denoted model 1 in Table 13.

5.3.2 ARIMA-GARCH - Temperature and Rain Restrictions

2 restrictions are imposed on the ARIMA-GARCH model with AR-lag 1, MA-lags 11, 26 and a GARCH(1,1). Model 2 is estimated without temperature, and model 3 is estimated without rainfall to capture possible effects on the system price and volatility. Results can be observed in Table 13 as model 1, with the model in Equation (G.1).

$$\begin{aligned} lnprice_t &= \alpha_0 + \beta' \mathbf{X}_t + \rho_1 lnprice_{t-1} \\ &+ \theta_2 u_{t-11} + \theta_4 u_{t-26} + \varepsilon_t \\ \varepsilon_t = \sigma_t^2 &= \alpha_0 + \alpha_1 u_{t-1}^2 + \gamma_1 \sigma_{t-1}^2 \end{aligned} \tag{G.1}$$

$\mathbf{X}$ is a vector of the regressors in Table 17, except lnprice and rvar.

ε_t defines the GARCH(1,1) specification of the ARIMA-GARCH.

Removal of MA(8,15) does not result in any noteworthy findings in terms of regression coefficients. However, AIC decreases from -2519.7211 to -2262.9085 and BIC decreased from -2146.8162 to -2159.0360. Thus, a model without MA(8,15) indicates an improved model specification. The model is denoted as 1 in Table 13. ARCH and GARCH effects are similar with a highly volatile system price including overall volatility persistence and non-stationary variance above 1, equal to 1.1496. Furthermore, statistically significant MA(11) and MA(26)-terms at a 1% significance level indicate the presence of quarterly and half-year seasonal effects.

5.3.3 ARIMA-GARCH - Without Temperature

Additionally, an ARIMA-GARCH model with AR-lag 1, MA-lags 11, 26 and a GARCH(1,1) without temperature is estimated and denoted as model 2 in Table 13, with specification in Equation (G.2). The main purpose is to determine if temperature in cities carry any

significance for the system price and volatility.

$$lnprice_t = \alpha_0 + \beta' \mathbf{X}_t + \rho_1 lnprice_{t-1}$$
$$+\theta_2 u_{t-11} + \theta_4 u_{t-26} + \varepsilon_t$$
$$\varepsilon_t = \sigma_t^2 = \alpha_0 + \alpha_1 u_{t-1}^2 + \gamma_1 \sigma_{t-1}^2 \qquad \texttt{(G.2)}$$

$\mathbf{X}$ is a vector of the regressors in Table 17, except lnprice, rvar, and temperatures.

ε_t defines the GARCH(1,1) specification of the ARIMA-GARCH.

Estimated rainfall coefficients, except for Bergen, are smaller against the ARIMA and ARIMA-GARCH models, implying that the effect of rainfall deviation on the system price is smaller when temperature is excluded. However, some effects are abnormally large with rainfall in Kr. Sand, Stavanger and Trondheim affecting the system price through 1 mm. increased rainfall deviation by ≈ -79.99%, ≈ 37.45% and ≈ 38.86%, respectively. Rainfall in Bergen now has an estimated effect of -16.91%, which is larger than both ARIMA-GARCH models (-16.61% `G.0`, -15.99% `G.1`) and smaller than the estimates from the preferred ARIMA model (-22.29% `A.3`). Rainfall estimates from Oslo have switched sign from the ARIMA estimation, with a smaller effect than all previous models at -0.86%. Rainfall in Bergen, Trondheim and Stavanger falls outside of a 5% significance level. From the model estimation, rainfall deviation including expectation and supply effects therefore has a smaller effect on the system price without temperature included.

The ARCH-term, α_1, decreases from 0.7488 to 0.7081, implying a 0.0407 reduction in volatility response from shocks today. On the other hand, the GARCH term, σ_1, has increased from 0.4008 to 0.4239, indicating a 0.0231 increase in correlation between volatility over two periods, and further evidence of volatility clustering. In summary, overall volatility persistence has decreased from 1.1496 to 1.1320, implying slightly less exponential volatility when excluding temperature, still non-stationary in variance. The model is still highly volatile. Quarterly and half-year seasonal effects remain present and statistically significant on a 1% significance level. Visual model fit based on a static in-sample forecast can be found in Figure 21.

AIC has decreased from -2262.9085 to -2270.1139 and BIC has decreased from -2159.0360 to -2193.3386. This is no surprise considering the previously statistically insignificant and small temperature effects. In conclusion, the ARIMA-GARCH model without temperature is proposed as superior to the ARIMA-GARCH with temperature included.

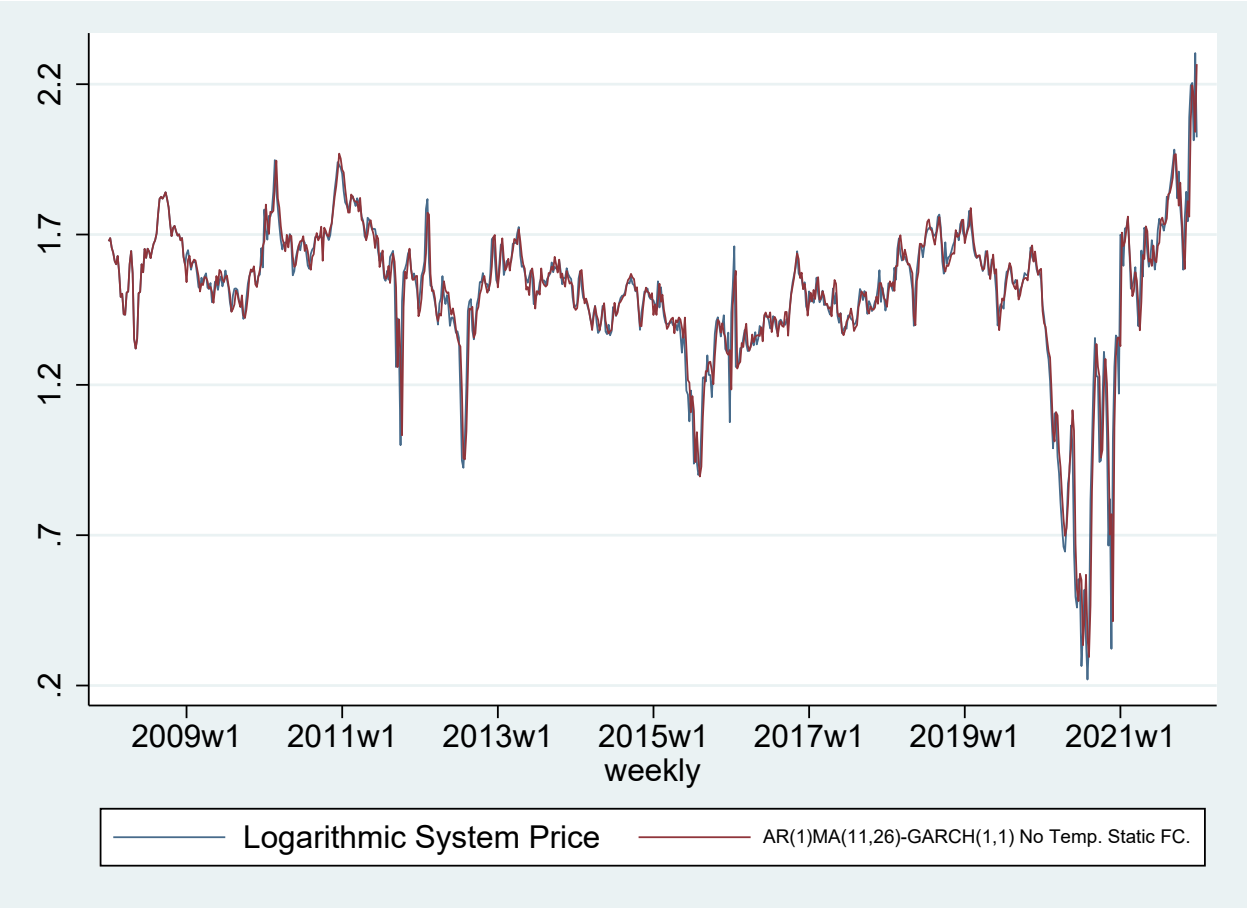

Figure 21: Visual model fit for the AR(1)MA(11,26)-GARCH(1,1) without temperature.

5.3.4 ARIMA-GARCH - Without Rainfall

Furthermore, an ARIMA-GARCH model with AR-lag 1, MA-lags 11, 26 and a GARCH(1,1) without rainfall is estimated to analyze effects on system price and volatility. Results can be observed in model 3 in Table 13 with equation written in Equation (G.3). Visual model

fit based on a static in-sample forecast can be found in Figure 22.

$$\begin{aligned} lnprice_t &= \alpha_0 + \beta' \mathbf{X}_t + \rho_1 lnprice_{t-1} \\ &+ \theta_2 u_{t-11} + \theta_4 u_{t-26} + \varepsilon_t \\ \varepsilon_t = \sigma_t^2 &= \alpha_0 + \alpha_1 u_{t-1}^2 + \gamma_1 \sigma_{t-1}^2 \end{aligned} \tag{G.3}$$

$\mathbf{X}$ is a vector of the regressors in Table 17, except lnprice, rvar and rainfall.

ε_t defines the GARCH(1,1) specification of the ARIMA-GARCH.

Temperature coefficients against model Equations (G.0) and (G.1) are generally larger, except for Stavanger which now has an estimated -0.6% effect on the system price against model (G.0) equal -0.2%, and model (G.1) equal -0.16%. Coefficients on Bergen and Tromsø have switched signs. Estimated effect in Bergen equal 0.36% against -0.59% (G.0) and -0.64% in (G.1). Estimated effect in Tromsø equals 2.85%, previously -0.15 % in (G.0) and -0.04% in (G.1). Temperature in Trondheim is now statistically significant at a 1% significance level; however, the coefficient equals a -0.12% reduction in system price, a marginal effect. Against the ARIMA model, estimates for Tromsø and Bergen are larger, whereas the other estimates are smaller.

However, the ARCH and GARCH-terms remain statistically significant. The ARCH-term has decreased by 0.082 compared to model 1 and 0.0413 compared to model 2, which indicates a less volatile system price from shocks today when excluding rainfall. Per contra, the GARCH-term has increased by 0.05 from model 1 and 0.0269 from model 2, indicating a higher correlation in variance over two periods, and additional volatility clustering. Overall volatility persistence has decreased from model 1 and 2 and equal 1.1176. The volatility persistence is therefore still exponential and non-stationary in variance, albeit to a slightly smaller degree. Quarterly and half-year seasonal effects remain present. In summary, excluding rainfall in this analysis results in a slightly less volatile system price.

AIC equal -2246.7818 and is larger than both model 1 and model 2, indicating a worse fit than prior. BIC however determines a better model fit than model 1, and a worse model fit than model 2. In summary, a model specification without temperature is proposed as

superior and further implies that temperature has little to no effect on the system price.

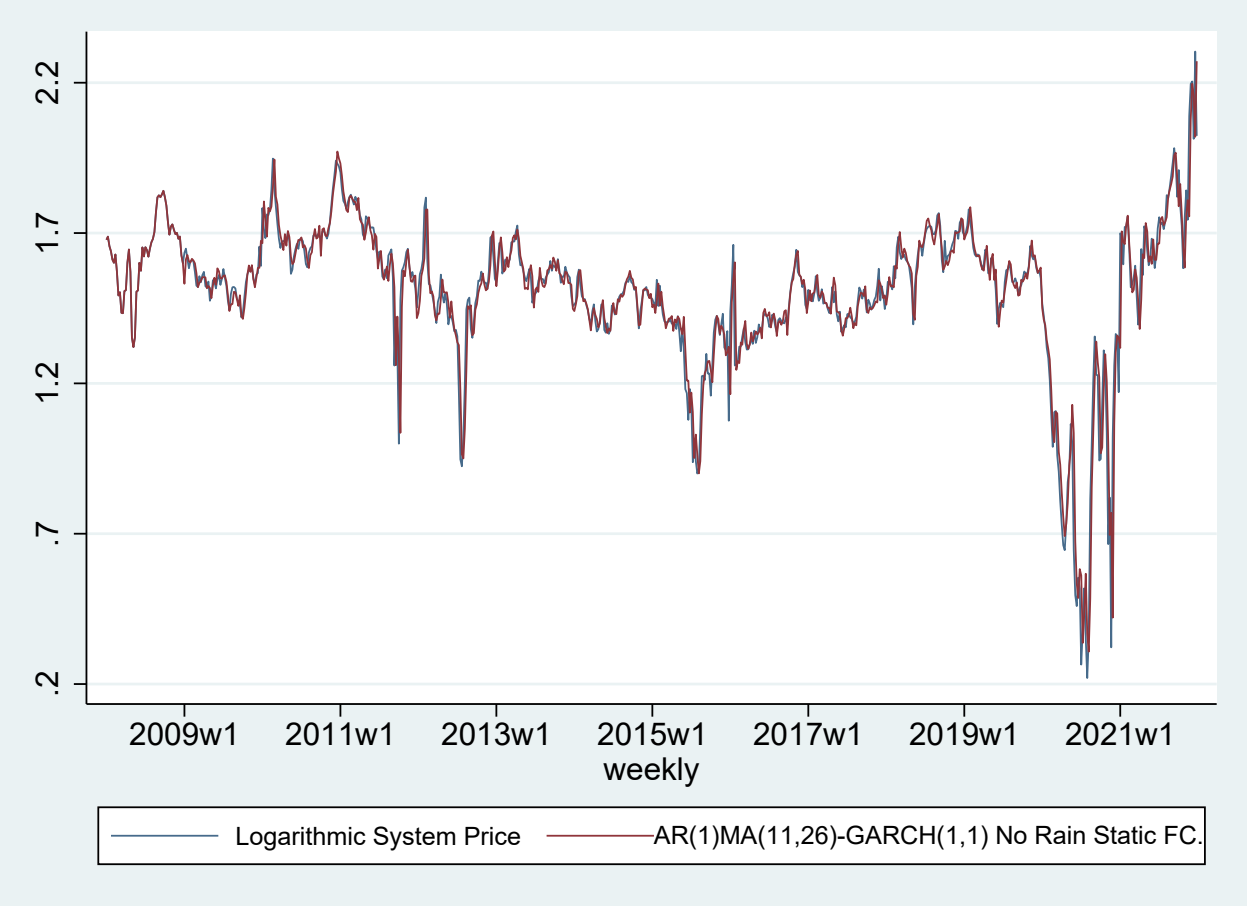

Figure 22: Visual model fit for the AR(1)MA(11,26)-GARCH(1,1) without rainfall.

5.3.5 Model Fit and In-Sample Properties

In-sample statistics can be observed in Table 8. Visual model fit for the ARIMA-GARCH variants can be observed in Figure 23, where all models follow the system price accurately. For the system price, Theil's U < 1 for all models. MAPE and RMSE favors the AR(1)MA(8,11,15,26)-GARCH(1,1), whereas MAE is a tie between the aforementioned ARIMA-GARCH and the AR(1)MA(11,26)-GARCH(1,1) without temperature. Against the preferred ARIMA model, forecasting errors are similar. The ARIMA model has a lower RMSE, MAPE and Theil's U, whereas the ARIMA-GARCH models have a lower MAE. Differences are, however, small. Nonetheless, when considering previous information criteria such as AIC and BIC it is difficult to determine the superior model.

Model	Obs	Theil	MAPE	MAE	RMSE
AR(1)MA(8,11,15,26)-GARCH(1,1), Price	676	0.8437	3.61%	0.0411	0.0738
AR(1)MA(11,26)-GARCH(1,1), Price	676	0.8408	3.63%	0.0412	0.0739
AR(1)MA(11,26)-GARCH(1,1) No Temp., Price	676	0.8487	3.62%	0.0411	0.0742
AR(1)MA(11,26)-GARCH(1,1) No Rain, Price	676	0.8396	3.65%	0.0416	0.0746
AR(1)MA(8,11,15,26)-GARCH(1,1), Vol	676	3.2642	400.1061%	0.0088	0.0298
AR(1)MA(11,26)-GARCH(1,1), Vol	676	3.1691	399.2418%	0.0088	0.0297
AR(1)MA(11,26)-GARCH(1,1) No Rain, Vol	676	4.0304	437.2231%	0.0087	0.0294
AR(1)MA(11,26)-GARCH(1,1) No Temp., Vol	676	3.0760	404.0892%	0.0088	0.0297

Table 8: ARIMA-GARCH variants forecasting accuracy statistics.

For the volatility, conditional variance from the ARIMA-GARCH models are compared to `rvar`, the realized variance as computed in Section 4.5.1. MAPE is above 400% for all models except the AR(1)MA(8,11,15,26)-GARCH(1,1). This might be due to skewness, low values of the variance or the over-influence of outliers. Additionally, Theil's U is > 1 in all cases, indicating a poor in-sample fit, worse than guessing. While this might be worrying, since both the numerator and denominator are means of squared percentage errors, Theils' U suffers from the same shortcomings as MAPE. MAE and RMSE leans towards the model without rain, however the differences between the ARIMA-GARCH models are diminutive, acting on the 4th decimal. Similar to the results for the system price it is therefore accordingly difficult to determine the superior model fit when assessing models through a statistical framework (Davydenko and Fildes, 2013; Enders, 2014; Brooks, 2019).

5.4 ARIMA-GARCH Robustness

To test whether the ARIMA-GARCH models are properly fitted, a residual analysis on standardized residuals is performed. First, standardized residuals are illustrated in a histogram with a normal frequency curve to visually inspect the distribution. Second, normality of the standardized residuals are tested with a Shapiro-Wilk normality test. Lastly, Barlett's periodogram-based test for white noise is applied, with both values and a cumulative periodogram for the standardized residuals.

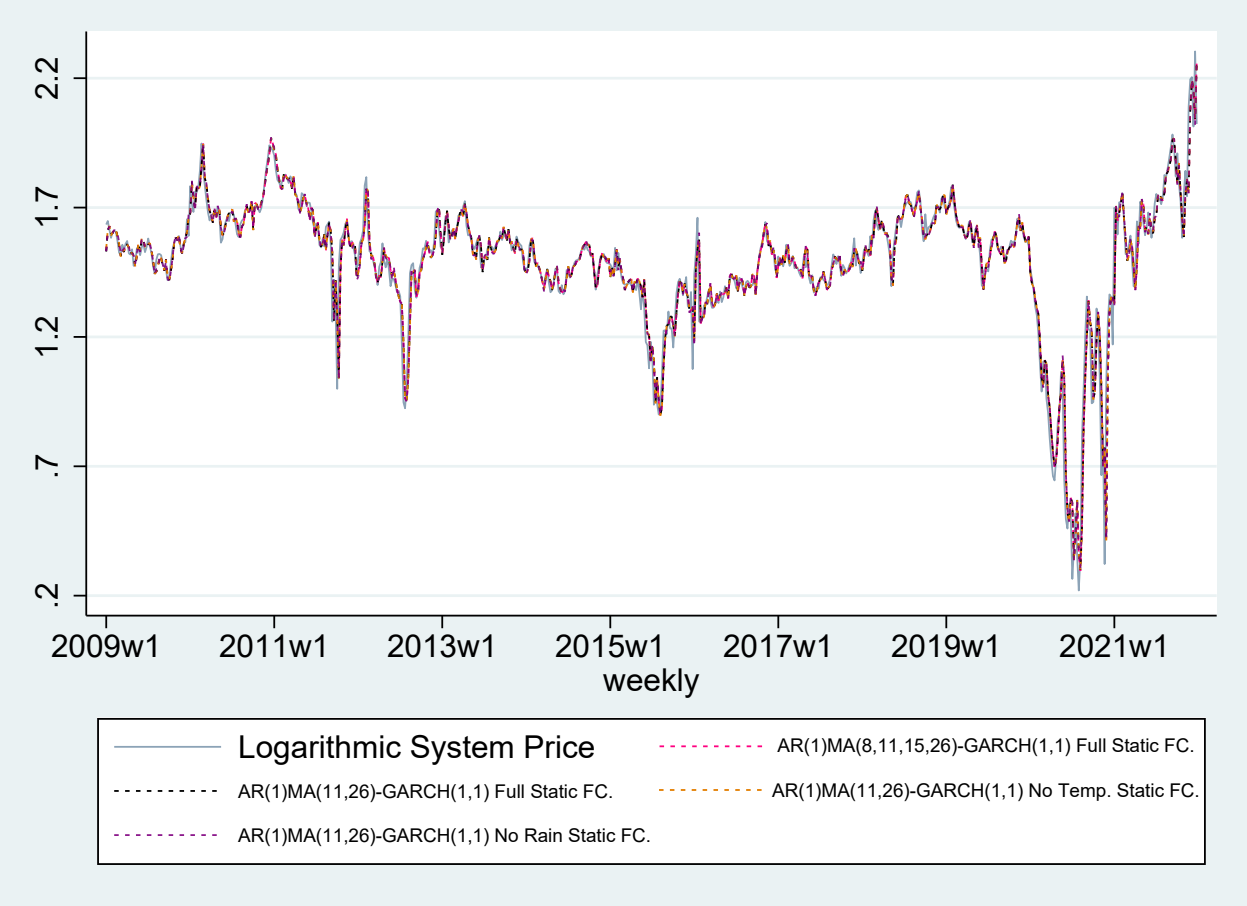

Figure 23: Visual model fit for the ARIMA-GARCH variants.

First and foremost, a standardized residual is calculated as in Equation (SR).

$$\hat{v_t} = \frac{\hat{u_t}}{\hat{\sigma_t}} \tag{SR}$$

Histograms with normal frequency curves can be observed in Figures 24 to 27 and summary statistics can be observed in Table 9. Histograms report a normal distribution with density around 0 for all 4 models and a slightly leptokurtic distribution for the AR(1)MA(11,26)-GARCH(1,1) variants. Observe from the summary statistics that all standardized residuals have a $N \sim (0, 1)$ distribution with outliers ranging from ≈ -6 to ≈ 8.

Shapiro-Wilk results can be found in Table 23, and test statistic can be observed in Equation (S-W TS) where x_i are ordered sample values, and a_i are a set of constants (Shapiro and Wilk, 1965). The formulated null and alternative hypothesis follow.

W H_0 : Normally distributed standardized residuals, follows $N \sim (\mu, \sigma^2)$.

W H_A : Non-normally distributed standardized residuals.

$$W = \frac{(\sum_{i=1}^{n} a_i x_i)^2}{\sum_{i=1}^{n}(x_i - \bar{x})^2} \qquad \texttt{(S-W TS)}$$

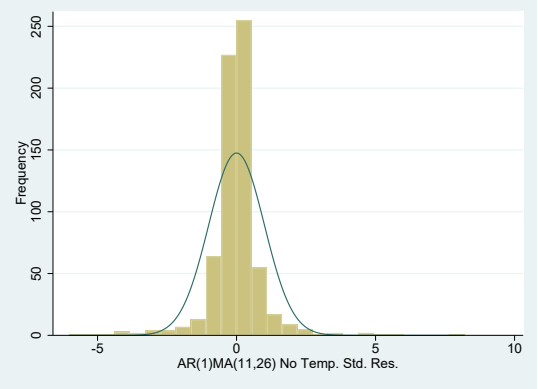

Figure 24: Standardized residual histogram with normal frequency for AR(1)MA(11,26)-GARCH(1,1). Without temperature.

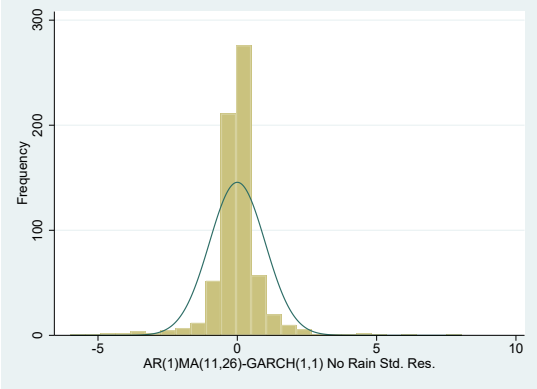

Figure 25: Standardized residual histogram with normal frequency for AR(1)MA(11,26)-GARCH(1,1). Without rainfall.

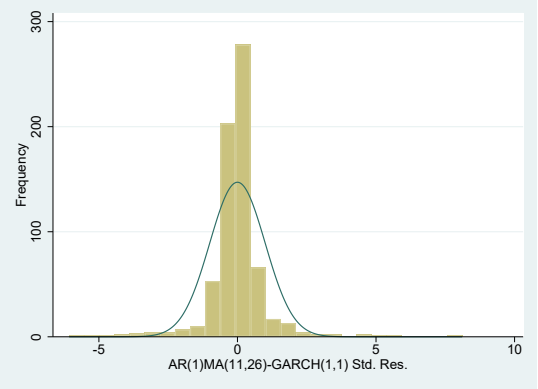

Figure 26: Standardized residual histogram with normal frequency for AR(1)MA(11,26)-GARCH(1,1).

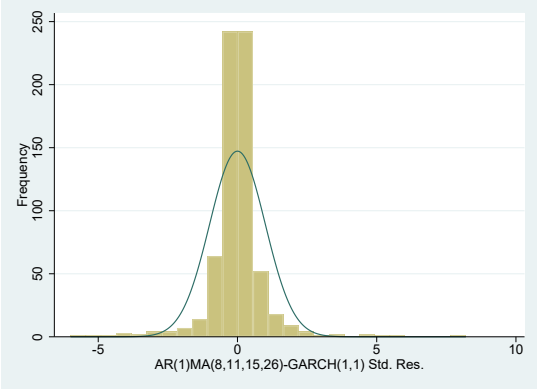

Figure 27: Standardized residual histogram with normal frequency for AR(1)MA(8,11,15,26)-GARCH(1,1).

Observing results from Table 23, the null hypothesis of normally distributed random residu-

als is rejected in all of the ARIMA-GARCH models. However, the parameter estimates will still be consistent, given a correct ARIMA-GARCH specification for the mean and variance (Brooks, 2019).

Lastly, Barlett's periodogram based test for white noise has been applied to the standardized residuals. The test statistic, along with the cumulative periodogram formula can be observed in Equation (B TS).

$$B = max_{1 \leq k \leq q} \sqrt{\frac{n}{2}} |\hat{F}_k - \frac{k}{q}|$$
$$\hat{F}_k = \frac{\sum_{j=1}^{k} \hat{f}(\omega_j)}{\sum_{j=1}^{q} \hat{f}(\omega_j)} \quad \text{(B TS)}$$

$\hat{F}_k$ = *cumulative periodogram defined in terms of the sample spectral density.*

Barlett's periodogram based test for white noise has the following null and alternative hypothesis:

B H_0 : White-noise process of uncorrelated random variables having a constant mean and a constant variance.
B H_A : Not white noise.

Results from Barlett's test conclude that the null hypothesis cannot be rejected in all ARIMA-GARCH specifications, indicating that the standardized residuals are not significantly different from a white noise process. Results can be found in Figures 37 to 40.

Variable	Obs	Mean	StdDev	Min	Max
AR(1)MA(11,26)-GARCH(1,1)	676	-0.0000	1.0000	-6.0746	8.1094
AR(1)MA(11,26)-GARCH(1,1) No Temp	676	-0.0000	1.0000	-6.0205	8.2014
AR(1)MA(11,26)-GARCH(1,1) No Rain	676	-0.0000	1.0000	-5.9887	8.0561

Table 9: Standardized residuals summary statistics for ARIMA-GARCH variants.

5.5 Discussion and Evaluation of Results

To further expand empirically and economically on relevant findings, this subsection examines results from the ARIMA and ARIMA-GARCH estimation procedure.

5.5.1 Seasonality

Within the ARIMA estimation, statistically significant MA parameters indicate 2-month, quarterly, 15-week and half-year seasonal effects. This effect is reduced to a quarterly and half-year effect when moving to the ARIMA-GARCH models. The finding is not very surprising, considering seasonal patterns previously mentioned in other articles, for instance by Koopman et al. (2007) and Bowden and Payne (2008). Inspecting ACF and PACF plots from residuals, further possible seasonal effects can be observed revealing a complex lag-structure beyond the scope of this dissertation, and the possibility of more complex seasonal effects. This includes ACF lags 4, 6, 7, 8, 15, 16, 34 and PACF lags 4, 6, 7, 8, 33, 43, 44, 56, 58, and further lags above 60. Observe Figures 29 to 32 which include ACF and PACF plots for the different ARIMA-GARCH models. The seasonality is empirically predictable. Considering aforementioned effects affecting the system price, water can be interpreted as a collection variable. Taking this into account, seasonally dependent effects such as temperature, weather, seasons, holidays, and trading patterns contribute to seasonality within the system price. For instance, electricity consumption during the winter in Nordic countries is larger than during the summer, affecting the demand for electricity positively, which can be captured through the half-year seasonal effect.

Furthermore, limited inflow to water magazines during the winter due to snowfall contributes to higher system prices. Per contra, increased inflow to water magazines in the summer contributes to lower system prices (NVE, 2020, 2021). The effects are captured in both the quarterly and half-year seasonal effects when considering winter and summer lengths. Quarterly and half-year seasonal effects should therefore be considered as a minimum, and results imply appreciable possibilities for a more complex seasonal lag-structure. For instance, by studying winter lengths in southern parts of the Nordic countries versus northern parts of the Nordic countries, more complex geographically dependent seasonal lag-lengths are probable,

suggesting a highly complex region dependent lag-structure.

5.5.2 Temperature Effects

As previously discussed, temperature has a small effect on the system price when included in the ARIMA or ARIMA-GARCH models. *Weighted* temperature is included to capture consumption and demand effects of population density and therefore functions as a proxy for regional consumer power demand. Higher temperature is expected to *reduce* electricity consumption, and lower temperatures are expected to *increase* power consumption[9]. This has high relevance in Norway, considering seasonal and regional differences in temperature. Results are consistent throughout the estimation process, both for population weight determination, ARIMA selection, and ARIMA-GARCH selection. This indicate that seasonally adjusted and population weighted temperatures have little to no effect on the system price and contribute more to model noise than to increasing the explanatory power. Throughout the ARIMA-GARCH modeling, the largest temperature effect is in Tromsø, equal to a 2.85% increase in system price. The temperature effect in Bergen, Kristiansand and Oslo also affect the system price positively. Effects in Trondheim and Stavanger are negative. Accordingly there are no demographic and geographical underlying effects within the variables to explain the system price. Therefore, the effects consumption, demand or temperature have on the system price can be declared as small, and statistically insignificant within the estimated models.

Furthermore, these small and statistically insignificant effects might be because the system price captures the Nordic countries, and since the cities in the dataset are not necessarily situated in close proximity to hydropower plants, or since temperature acts as a moving average, already included in ARIMA and ARIMA-GARCH models. Nonetheless, this is an interesting discovery. Furthermore, a likelihood-ratio test on temperature effects is performed to test whether temperature effects are nested within the fully specified ARIMA-GARCH. Results can be found in Table 10 which determines that temperature restrictions are jointly insignificant at a 57.04% significance level, which implies that seasonally adjusted and population

[9]For example at NVE (NVE, 2020, 2021).

weighted temperature for all 6 cities does not jointly contribute to explain the system price and volatility. In summary, temperature as included in this thesis does not affect the system price and does not contribute to explaining the system price in any statistically, empirically or economically meaningful way.

5.5.3 Rainfall Effects

Overall, a similar conclusion can be used to describe the results for weighted seasonally adjusted rainfall. *Weighted* rainfall is included to capture both expectation effects of population density and supply effects. Increased rainfall deviation is expected to *reduce* the system price. Furthermore, increased rainfall in a densely populated area such as Oslo, might contribute to expectations of a reduced electricity price to a higher degree than increased rainfall in a city with a lower population like Tromsø. However, throughout the analysis this is not the result which indicates that proximity to hydropower plants is more important than expectation and supply effects within the cities, in turn explaining statistical insignificance in Oslo. Contrasting and switching signs on coefficients, including awkward estimates produce an ambiguous effect on the system price, and applying regional electricity prices alongside rainfall or including extreme weather frequency might yield more precise estimates. Estimated effect for Oslo in the ARIMA-GARCH which excludes temperature equals a 0.86% reduction in the system price from rainfall deviation, whereas the effect equals a system price reduction of 0.05% by increased rainfall deviation in Tromsø. Isolated, these effects imply a very slight population weighted expectation and supply effect, but similar conclusions cannot be established for any other rainfall variables, invalidating the effect. In summary, this entails that the system price and volatility is more dependent on physical and fundamental effects, rather than population-bound effects. Considering these results, using magazine filling levels, magazine deviation, or hydrological balance in a similar way as Koopman et al. (2007) might give better results.

Nonetheless, the proposed model includes weighted and seasonally adjusted rainfall. Although the direct effect of rainfall on magazine levels is small, rainfall deviation in Bergen for instance provides somewhat meaningful results. Considering Bergen averages approxi-

mately 200 days of rainfall in a year, the probability of rainfall in Bergen coinciding with magazine levels is high (YR, 2019). However, since rainfall has been adjusted for population and seasonality, the effect carries less concern than including rainfall alone. Information criteria in terms of AIC and BIC favours the model with rainfall. Furthermore, a likelihood-ratio test on rainfall effects is performed to test whether rainfall effects are nested within the fully specified ARIMA-GARCH. Results can be found in Table 10 which determine that rainfall is jointly significant at a 0.02% significance level. This implies that seasonally adjusted and population weighted rainfall for all 6 cities jointly contributes to explain system price and volatility. In summary, rainfall does contribute statistically to explaining the system price, and does somewhat contribute empirically to explain the volatility of the system price. However, the effect is ambiguous (NVE, 2020, 2021).

Model	$\chi^2_{0.05}$	LR test statistic	Degrees of freedom	P-value
Temperature	12.592	4.7946	6	57.04%
Rainfall	14.067	28.1620	7	0.02%

Table 10: LR-test for rain and temperature restrictions.

5.5.4 Wind Power Production, Snow, Ground and Surface Water, and Magazine Deviation

Logarithmic wind power production, the sum of snow, ground and surface water and the sum of magazine deviation are persistently statistically significant on a 5% significance level. Magazine deviation capture deviations from the average influx to water magazines, aggregated to a national deviation from average. Sum of snow, ground and surface water capture indirect influx to water magazines. For instance, snow-melting due to higher temperatures or large amounts of surface water due to heavy rainfall results in increased indirect influx to water magazines.

An increase in the sum of snow, ground and surface water contributes to a lower system price, and a positive increase in the sum of magazine deviation also contributes to a lower system price, ceteris paribus. This is an expected finding since both variables contribute

to a higher magazine filling level through direct or indirect influx. Magazine deviation contributes to a reduced system price through increased rainfall at water magazines, whereas the sum of snow, ground and surface water contributes to a reduced system price through either increased rainfall in close proximity to water magazines or due to increased snow-melting, for instance through higher temperatures. The effect of magazine deviation is larger than the sum of snow, ground and surface water, which implies that the direct effect of rainfall is larger than the indirect effect of rainfall and temperature. Increased wind power production is also expected to reduce the system price through a higher level of electricity supplied to the market. The effect of wind power production on the system price will likely increase in the following years, considering both trends, forecasts, signals from Nordic government, and discussions with power market traders[10] (Regjeringen, 2019). In summary, the sum of magazine deviation, the sum of snow, ground and surface water, and logarithmic wind power production does contribute to explain both the system price and its volatility. Results are comparable to Koopman et al. (2007), who apply magazine filling levels, but are taken a step further by including wind power production and sum of snow, ground and surface water (NVE, 2020, 2021)

5.5.5 Autoregressive System Price

Throughout the estimation procedure, the AR(1) coefficient has been consistently above 0.9 for the ARIMA-GARCH models and statistically significant on all relevant significance levels, which are similar to results obtained by Koopman et al. (2007). The results are close to a unit root process, which implies that the system price is highly dependent on the system price in the previous week. Contemplating previous rejection of a unit root, this is an interesting finding, which should be discussed further. A feature of the Norwegian power system is that a substantial proportion of the power production comes from hydropower production. Considering underlying features of the hydropower system, the price is highly dependent upon weekly reported magazine filling levels in the short run, together with expected water inflow and electricity demand. These variables therefore determine the alternative costs for water, and express levels retained over a shorter period when observing the system price at

[10]Discussion with power market traders at Tussa Energi in February.

a higher frequency such as weekly. It is therefore expected that the system price on a weekly basis is highly autoregressive despite rejection of a unit root (Statnett, 2022).

5.5.6 ARCH and GARCH Terms

ARCH and GARCH-terms are persistently statistically significant on all relevant significance levels and encapsulates the highly volatile nature of the system price. In all ARIMA-GARCH models the sum of ARCH and GARCH coefficients are above 1, indicating exponential volatility persistence in all cases and non-stationarity in variance. The volatility persistence is slightly lower for the ARIMA-GARCH without temperature, and the lowest for the ARIMA-GARCH without rainfall compared to the ARIMA-GARCH without any restrictions, indicating that rainfall contributes more to explaining volatility persistence than temperature.

Furthermore, the ARIMA-GARCH model without rainfall reacts less to shocks in volatility than the other ARIMA-GARCH models, but with a higher correlation in variance over two periods. The ARIMA-GARCH without temperature has a greater response to shocks in volatility than the ARIMA-GARCH without rainfall, but with a lower correlation in variance over two periods. This is unsurprising, since rainfall can occur in bursts, for instance during extreme weather conditions, while temperature follow averages more closely. However, temperature deviations do occur. High temperatures can contribute to increased snow melting and evaporation, whereas cold temperatures can contribute to increased power demand and consumption, affecting the volatility of the system price. These effects contribute to more volatility clustering than rainfall, implying that rainfall has a slightly larger effect on contemporaneous and short-run volatility, whereas temperatures have a slightly larger effect on long-run volatility. In summary, excluding temperature or rainfall does not hold any major effect on the volatility, but the ARIMA-GARCH without rainfall captures less volatility persistence than the model without temperature, probably due to aforementioned effects. The unrestricted model is the most volatile.

Figure 28 illustrates the realized variance against the AR(1)MA(11,26)-GARCH(1,1) vari-

ants for the conditional variance. The 3 different ARIMA-GARCH models capture the trend of the realized variance well, but fail to fully capture large spikes in volatility, for example around week 1, 2021. However, the fully specified ARIMA-GARCH visually conveys the impression of advantageous volatility capture. Visual results imply that there might be other effects apart from rainfall, temperature, and other explanatory variables included in the dissertation which affect the volatility of the system price. This likely reflects the fact that the system price captures all bids and offers within the Nordic market. Future research on the topic should therefore consider including the power mix in additional countries. Furthermore, realized variance may be subject to noise and including other volatility measures such as implied variance might yield other results.

5.5.7 Structural Breaks and Asymmetry

It should be mentioned that the system price exhibits evidence of structural breaks. A parameter stability test through a cumulative sum of recursive residuals was performed with evidence of parameter instability between 2016 to early 2018, and in 2020. Empirically, this instability was most likely due to temporary limited exporting capacities, low costs, and domestic effects, suggesting a regime shift, rather than a structural break (Farmer, 2022). Therefore, use of regime switching models such as the Markov-Switching class may be appropriate for future extensions (NVE, 2020).

Another class of GARCH models that could have been adopted is GARCH models that allow for asymmetric volatility responses, such as the EGARCH. An Engle-NG test for asymmetry was performed, which confirmed the presence of leverage effects. Future extensions on the topic should therefore consider appending the analysis with models that allows for asymmetric responses, such as Liu and Shi (2013); Bowden and Payne (2008) or Cifter (2013). Neither regime-switching nor asymmetries have been explicitly modeled in the dissertation, due to the scope of the thesis statement, time, and space restrictions. However, the performed tests deliver intriguing results for further research.

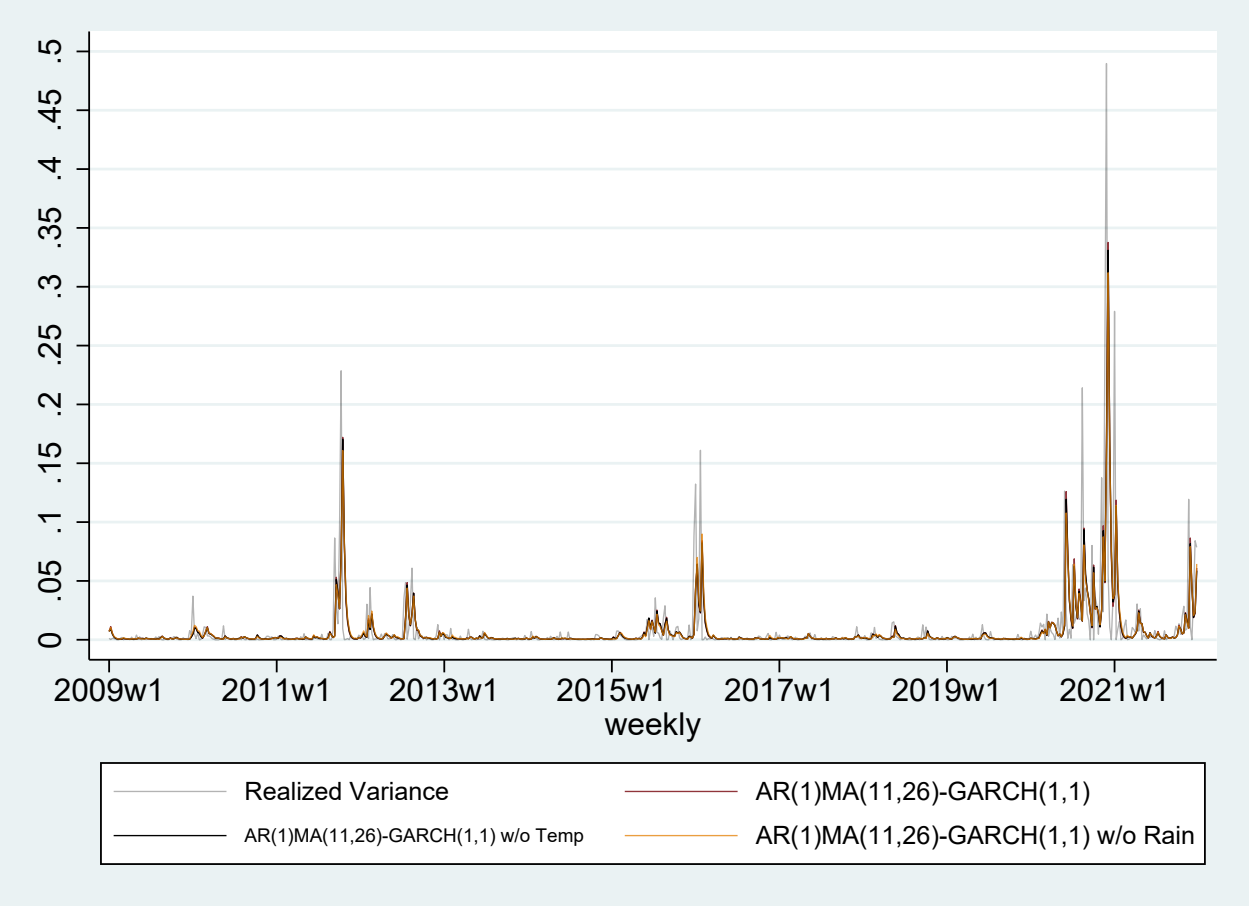

Figure 28: Visual model fit for the ARIMA-GARCH Variants for conditional volatility against realized variance.

6 Conclusion

Electricity prices are subject to high volatility. The dissertation has studied the system price at Nord Pool between week 1, 2008 through week 52, 2021 which has revealed a highly volatile system price. The main focus of the dissertation was to study:

1. To what extent does population weighted and seasonally adjusted temperature and rainfall affect system price and volatility?
2. Which other effects affect system price and volatility?

In summary, temperature has a minor effect on the system price. The effects consumption, demand or temperature have on the system price can be declared as small, and statistically

insignificant within the estimated models. Rainfall, expectation and supply effects does contribute slightly to explain the system price and are statistically significant. Both temperature and rainfall contribute slightly in explaining volatility. Other effects including magazine deviation, snow, surface, and groundwater, wind power production, seasonal effects and the autoregressive effect of order 1 contribute to explain the system price and volatility.

Previous studies using ARIMA or ARIMA-GARCH models have been conducted, however, few studies have explicitly modeled other effects affecting electricity prices, and the effect they have on volatility. To expand research on electricity prices and volatility, the dissertation has therefore considered several effects which possibly affect the system price and volatility. Temperature and rainfall from 6 cities in Norway were included, seasonally adjusted, and population weighted to capture expectation, supply, consumption and demand effects including temperature and rainfall deviation. Additionally, wind power production, magazine deviation and influx to water magazines through the sum of snow, ground and surface water were included to investigate additional effects on the system price and volatility.

Throughout the dissertation various ARIMA and ARIMA-GARCH models have been fitted and estimated. Firstly, a set of ARIMA models were estimated to determine optimal lag-length while pursuing parsimony through the 3-step Box-Jenkins approach. Results concluded with an ARIMA model with AR-lag 1, and MA-lags 8, 11, 15 and 26 as the preferred model. ARIMA model fitting revealed a complex seasonal pattern and lag structure, where some lags were excluded to persevere parsimony. Moreover, population weights for seasonally adjusted temperature and rainfall were determined through the preferred ARIMA model. Population weights determined through dataset population and therein population in the 6 cities was the preferred method due to collinearity. Next, a GARCH(1,1) was appended on the ARIMA model, including a correction of lag-length. Due to insignificant MA-terms, an ARIMA-GARCH with AR-lag 1 and MA-lags 11 and 26, including a GARCH(1,1) process was chosen. The ARIMA-GARCH model was estimated with restrictions on seasonally adjusted and population weighted rainfall and temperature. All ARIMA-GARCH models followed the trend of the system price and volatility well.

Somewhat surprisingly, seasonally adjusted and population weighted temperature and rainfall had little to no effect on the system price, and a marginal effect on volatility. Temperature in the 6 cities over the 14-year estimation period resulted in no evidence of an consumption- or demand effects of any relevance. Coefficient estimates were small, statistically insignificant and difficult to interpret. Furthermore, there is little evidence of seasonally adjusted and population weighted rainfall affecting the system price. Considering rainfall has a direct empirical effect on magazine filling levels it was somewhat surprising that only estimates from Bergen had statistical and empirical significance. The effect was therefore determined ambiguous and imprecise. Accordingly, expectation, supply, consumption and demand effects had impractical results and subsequent temperature and rainfall effects were not affecting the system price in any noteworthy way. Results throughout the estimation procedure revealed a highly autoregressive system price of order 1 despite rejection of a unit root process in all variables. A reasoning considering underlying features of the Norwegian hydropower system concluded with empirically predictable results. Quarterly, and half-year seasonal effects were found in the ARIMA-GARCH model. Considering the complex lag-structure by studying ACF and PACF, more complex seasonal patterns are probable and consistent with previously reviewed literature. Wind power production, snow, ground and surface water, and magazine deviation were statistically significant throughout the estimation procedure. Accordingly, increased wind power production, increased inflow to water magazines and increased positive magazine deviation were all expected to reduced the system price.

ARCH and GARCH terms were consistently statistically significant throughout the ARIMA-GARCH estimation procedure. Evidence of exponential volatility and non-stationary variance was found, regardless of model specification, with the sum of ARCH and GARCH coefficients above 1 in all estimated models. This was consistent with literature previously reviewed. Volatility persistence was the highest for the fully specified model, followed by the model without temperature, and lastly the model without and rainfall. The unrestricted model had the highest response to volatility shocks through the ARCH term, followed by the model without temperature and the model without rainfall. The model without rainfall had the highest correlation in variance over two periods, followed by the model without temperature and lastly the unrestricted model. Results were likely due to temperature acting as a

moving average and rainfall occurring in bursts. In summary, rainfall had a slightly larger effect on contemporaneous and short-run volatility, whereas temperatures had a slightly larger effect on long-run volatility.

All estimated models followed the volatility measure as calculated through realized variance, `rvar`, but failed to fully capture spikes in volatility. This might be due to model specification, or an imprecise measure of volatility. Lastly, evidence of structural breaks and asymmetric volatility response was found. Future research should therefore consider including Markow-switching (MS) and GARCH specifications that capture asymmetry.

Bibliography

Tim Bollerslev. Generalized autoregressive conditional heteroskedasticity. *Journal of Econometrics*, 31(3):307–327, 1986. ISSN 0304-4076. doi: https://doi.org/10.1016/0304-4076(86)90063-1. URL https://www.sciencedirect.com/science/article/pii/0304407686900631.

Silvano Bordignon, Massimiliano Caporin, and Francesco Lisi. Generalised long-memory garch models for intra-daily volatility. *Computational Statistics & Data Analysis*, 51(12):5900–5912, 2007. ISSN 0167-9473. doi: https://doi.org/10.1016/j.csda.2006.11.004. URL https://www.sciencedirect.com/science/article/pii/S0167947306004257.

Nicholas Bowden and James E. Payne. Short term forecasting of electricity prices for miso hubs: Evidence from arima-egarch models. *Energy Economics*, 30(6):3186–3197, 2008. ISSN 0140-9883. doi: https://doi.org/10.1016/j.eneco.2008.06.003. URL https://www.sciencedirect.com/science/article/pii/S0140988308000868. Technological Change and the Environment.

Chris Brooks. *Introductory Econometrics for Finance*. Cambridge University Press, 4. edition, 2019. doi: 10.1017/9781108524872.

Atilla Cifter. Forecasting electricity price volatility with the markov-switching garch model: Evidence from the nordic electric power market. *Electric Power Systems Research*, 102:61–67, 2013. ISSN 0378-7796. doi: https://doi.org/10.1016/j.epsr.2013.04.007. URL https://www.sciencedirect.com/science/article/pii/S0378779613001016.

Andrey Davydenko and Robert Fildes. *Measuring Forecasting Accuracy: Problems and Recommendations (by the Example of SKU-Level Judgmental Adjustments)*. Springer Heidelberg New York Dordrecht London, 10 2013. ISBN 978-3-642-39868-1. doi: 10.1007/978-3-642-39869-8_4.

Theodore E. Day and Craig M. Lewis. Stock market volatility and the information content of stock index options. *Journal of Econometrics*, 52(1):267–287, 1992. ISSN 0304-4076. doi: https://doi.org/10.1016/0304-4076(92)90073-Z. URL https://www.sciencedirect.com/science/article/pii/030440769290073Z.

Olga Efimova and Apostolos Serletis. Energy markets volatility modelling using garch. *Energy Economics*, 43:264–273, 2014. ISSN 0140-9883. doi: https://doi.org/10.1016/j.eneco.2014.02.018. URL https://www.sciencedirect.com/science/article/pii/S0140988314000486.

Graham Elliott, Thomas J. Rothenberg, and James H. Stock. Efficient tests for an autoregressive unit root. *Econometrica*, 64(4):813–836, 1996. ISSN 00129682, 14680262. URL http://www.jstor.org/stable/2171846.

Walter Enders. *Applied Econometric Time Series*. Wiley, 4. edition, 2014. ISBN ISBN: 978-1-118-80856-6.

Matt Farmer. How norway became europe's biggest power exporter, 2022. URL https://www.power-technology.com/features/how-norway-became-europes-biggest-power-exporter/. Accessed: 14.03.2022.

Michael Frömmel, Xing Han, and Stepan Kratochvil. Modeling the daily electricity price volatility with realized measures. *Energy Economics*, 44:492–502, 2014. ISSN 0140-9883. doi: https://doi.org/10.1016/j.eneco.2014.03.001. URL https://www.sciencedirect.com/science/article/pii/S0140988314000425.

Peter R. Hansen and Asger Lunde. A forecast comparison of volatility models: Does anything beat a garch(1,1)? *Journal of Applied Econometrics*, 20(7):873–889, 2005. ISSN 08837252, 10991255. URL http://www.jstor.org/stable/25146403.

Erik Holmqvist. Beregning av energitilsig basert på hbv-modeller. *NVEs hustrykkeri*, 30(29), 2013.

Siem Jan Koopman, Marius Ooms, and M. Angeles Carnero. Periodic seasonal reg-arfima-garch models for daily electricity spot prices. *Journal of the American Statistical Association*, 102(477):16–27, 2007. ISSN 01621459. URL http://www.jstor.org/stable/27639816.

Heping Liu and Jing Shi. Applying arma–garch approaches to forecasting short-term electricity prices. *Energy Economics*, 37:152–166, 2013. ISSN 0140-9883. doi: https://

doi.org/10.1016/j.eneco.2013.02.006. URL https://www.sciencedirect.com/science/article/pii/S0140988313000303.

Robert Nau. Statistical forecasting: notes on regression and time series analysis. https://people.duke.edu/~rnau/411home.htm, 2020. Accessed: 09.03.2022.

NordPool. Nordic system price, methodology for calculation, 2020. URL https://www.nordpoolgroup.com/4a7544/globalassets/download-center/day-ahead/methodology-for-calculating-nordic-system-price.pdf. Accessed: 01.05.2022.

NordPool. Price calculation, 2022. URL https://www.nordpoolgroup.com/trading/Day-ahead-trading/Price-calculation/. Accessed: 02.03.2022.

NVE. Kraftsituasjonen - fjerde kvartal og året 2020. *Rapporter - Kraftsituasjonen*, 4:2, 2020. URL https://www.nve.no/media/11490/kraftsituasjonenq4.pdf.

NVE. Kraftsituasjonen - uke 50 2021. *Rapporter - Kraftsituasjonen*, 50:20, 2021. URL https://www.nve.no/media/13197/2021_50_kraftsituasjonen.pdf.

Jian-Xin Pan and Kai-Tai Fang. *Maximum Likelihood Estimation*, pages 77–158. Springer New York, New York, NY, 2002. ISBN 978-0-387-21812-0. doi: 10.1007/978-0-387-21812-0_3. URL https://doi.org/10.1007/978-0-387-21812-0_3.

Regjeringen. Olje- og energidepartementet, meld. st. 28 (2019–2020), vindkraft på land — endringer i konsesjonsbehandlingen. https://www.regjeringen.no/no/dokumenter/meld.-st.-28-20192020/id2714775/?ch=5, 2019. Accessed: 20.04.2022.

Stephan Schlueter. A long-term/short-term model for daily electricity prices with dynamic volatility. *Energy Economics*, 32(5):1074–1081, 2010. ISSN 0140-9883. doi: https://doi.org/10.1016/j.eneco.2010.06.008. URL https://www.sciencedirect.com/science/article/pii/S0140988310001040.

Samuel Sanford Shapiro and Martin B Wilk. An analysis of variance test for normality (complete samples). *Biometrika*, 52(3/4):591–611, 1965.

Ingve Simonsen. Volatility of power markets. *Physica A: Statistical Mechanics and its Applications*, 355:10–20, 09 2005. doi: 10.1016/j.physa.2005.02.062.

SSB. Population data. https://www.ssb.no/a/english/aarbok/emne02_main.html, 2013. Accessed: 01.03.2022.

Stata. estat ic - display information criteria, 2022. URL https://www.stata.com/manuals/restatic.pdf. Accessed: 23.02.2022.

Statkraft. Vannkraft (samleside), 2022. URL https://www.statkraft.no/var-virksomhet/vannkraft/. Accessed: 03.05.2022.

Statnett. Kraftmarkedet (samleside), 2022. URL https://www.statnett.no/for-aktorer-i-kraftbransjen/systemansvaret/kraftmarkedet/. Accessed: 01.04.2022.

Arve Tvede. Vannkraft i hordaland. https://www.grind.no/industri-energi-naturressursar/vannkraft-i-hordaland, 2017. From UiB, Accessed: 01.03.2022.

YR. Her regner det 200 dager i året. https://www.yr.no/artikkel/her-regner-det-200-dager-i-aret-1.14485816, 2019. Accessed: 20.04.2022.

A Model Estimates

A.1 Table 11: ARIMA Population Weight Model Estimates

Variable	(No Weights)	(Nat. Weights)	(City Weights)
S.Adj. Temp. Bergen	0.0066	0.1521	-0.0081
	(0.0057)	(0.0004)	(0.5809)
S.Adj. Temp. Kr. Sand	-0.0024	-0.0888	0.0177
	(0.2430)	(0.4138)	(0.6171)
S.Adj. Temp. Oslo	-0.0032	-0.0270	0.0206
	(0.0665)	(0.0543)	(0.1516)
S.Adj. Temp. Tromsø	0.0002	Col.	0.0097
	(0.8415)		(0.9224)
S.Adj. Temp. Trd.	-0.0003	-0.0066	-0.0017
	(0.8191)	(0.8705)	(0.0608)
S.Adj. Temp. Stvg.	-0.0047	-0.2828	-0.0031
	(0.0447)	(0.0000)	(0.7365)
S.Adj. Rain Trd.	0.1799	0.2291	0.4420
	(0.5152)	(0.4138)	(0.3775)
S.Adj. Rain Tromsø	-0.0016	-0.0017	-0.0043
	(0.3102)	(0.2855)	(0.0538)
Log. Wind Prod.	-0.0194	-0.0195	-0.0214
	(0.0214)	(0.0231)	(0.0172)
Sum Magazine Deviation	-0.0197	-0.0198	-0.0204
	(0.0000)	(0.0000)	(0.0000)
Sum Sno., Gro., Sur. Watr	-0.0105	-0.0108	-0.0104
	(0.0000)	(0.0000)	(0.0000)

Dummy=1, 2020	-0.2524	-0.2549	-0.2436
	(0.0000)	(0.0000)	(0.0000)
AR(1)	0.8864	0.8801	0.8769
	(0.0000)	(0.0000)	(0.0000)
MA(8)	0.1652	0.1763	0.1578
	(0.0000)	(0.0000)	(0.0000)
MA(11)	-0.1507	-0.1320	-0.1202
	(0.0000)	(0.0000)	(0.0001)
MA(15)	0.0942	0.1070	0.1085
	(0.0099)	(0.0101)	(0.0106)
MA(26)	-0.1476	-0.1648	-0.1756
	(0.0000)	(0.0000)	(0.0000)
S.Adj. Rain Oslo	Col.	0.0030	0.0060
		(0.8747)	(0.7642)
S.Adj. Rain Bergen	Col.	Col.	-0.2229
			(0.0865)
S.Adj. Rain Kr. Sand	Col.	Col.	-2.5348
			(0.0519)
S. Adj. Rain Stvg.	Col.	Col.	0.4671
			(0.4282)
AIC	-1686.9521	-1676.6916	-1663.2977
BIC	-1601.3138	-1590.8839	-1559.4253
Log likelihood	862.4760	857.3458	854.6489

Table 11: AR(1) MA(8,11,15,26) Estimates with different population weights. P-values in parenthesis.

A.2 Table 12: ARIMA Model Estimates

Variable	(1)	(2)	(3)
S.Adj. Temp Bergen	-0.0080	-0.0080	-0.0081
	(0.5912)	(0.5878)	(0.5809)
S.Adj. Temp Kr.Sand	0.0177	0.0177	0.0177
	(0.6163)	(0.6163)	(0.6171)
S.Adj. Temp Oslo	0.0204	0.0204	0.0206
	(0.1531)	(0.1527)	(0.1516)
S.Adj. Temp Tromsø	0.0104	0.0104	0.0097
	(0.9176)	(0.9175)	(0.9224)
S.Adj. Temp Trondheim	-0.0016	-0.0016	-0.0017
	(0.0680)	(0.0678)	(0.0608)
S.Adj. Temp Stvg.	-0.0032	-0.0032	-0.0031
	(0.7338)	(0.7335)	(0.7365)
S.Adj. Rain Bergen	-0.2246	-0.2247	-0.2229
	(0.0837)	(0.0834)	(0.0865)
S.Adj. Rain Kr.Sand	-2.5265	-2.5271	-2.5348
	(0.0531)	(0.0527)	(0.0519)
S.Adj. Rain Oslo	0.0060	0.0060	0.0060
	(0.7661)	(0.7637)	(0.7642)
S. Adj. Rain Stvg.	0.4685	0.4691	0.4671
	(0.4293)	(0.4259)	(0.4282)
S.Adj. Rain Tromsø	-0.0043	-0.0043	-0.0043
	(0.0539)	(0.0535)	(0.0538)
S.Adj. Rain Trondheim	0.4340	0.4340	0.4420
	(0.3865)	(0.3821)	(0.3775)
Log. Wind Prod.	-0.0213	-0.0213	-0.0214
	(0.0178)	(0.0177)	(0.0172)

Dummy=1, 2020	-0.2451	-0.2449	-0.2436
	(0.0000)	(0.0000)	(0.0000)
Sum Sno., Gro., Sur. wtr.	-0.0104	-0.0104	-0.0104
	(0.0000)	(0.0000)	(0.0000)
Sum Magazine Deviation	-0.0204	-0.0204	-0.0204
	(0.0000)	(0.0000)	(0.0000)
AR(1)	0.8795	0.8795	0.8769
	(0.0000)	(0.0000)	(0.0000)
AR(8)	-0.0095	-0.0095	
	(0.6084)	(0.6088)	
AR(26)	0.0003		
	(0.9885)		
MA(8)	0.1649	0.1649	0.1578
	(0.0000)	(0.0000)	(0.0000)
MA(11)	-0.1149	-0.1149	-0.1202
	(0.0020)	(0.0020)	(0.0001)
MA(15)	0.1105	0.1105	0.1085
	(0.0126)	(0.0112)	(0.0106)
MA(26)	-0.1744	-0.1741	-0.1756
	(0.0000)	(0.0000)	(0.0000)
AIC	-1659.4367	-1661.4365	-1663.2977
BIC	-1546.5319	-1553.0479	-1559.4253
Log likelihood	854.7183	854.7182	854.6489

Table 12: 1: AR(1,8,26)MA(8,11,15,26). 2: AR(1,8)MA(8,11,15,26). 3:AR(1)MA(8,11,15,26). P-values in parenthesis.

A.3 Table 13: ARIMA-GARCH Model Estimates

Variable	(0)	(1)	(2)	(3)
S.Adj. Temp Bergen	-0.0059	-0.0064		0.0036
	(0.2849)	(0.2408)		(0.2483)
S.Adj. Temp Kr.Sand	0.0100	0.0114		0.0137
	(0.5297)	(0.4740)		(0.3606)
S.Adj. Temp Oslo	0.0067	0.0064		0.0038
	(0.3151)	(0.3238)		(0.4926)
S.Adj. Temp Tromsø	-0.0015	-0.0004		0.0285
	(0.9723)	(0.9930)		(0.4414)
S.Adj. Temp Trondheim	-0.0003	-0.0003		-0.0012
	(0.6045)	(0.5160)		(0.0059)
S.Adj. Temp Stavanger	-0.0020	-0.0016		-0.0006
	(0.5836)	(0.6445)		(0.8652)
S.Adj. Rain Bergen	-0.1661	-0.1599	-0.1691	
	(0.0009)	(0.0014)	(0.0002)	
S.Adj. Rain Kr. Sand	-1.0363	-0.9924	-0.7977	
	(0.1371)	(0.1441)	(0.2398)	
S.Adj. Rain Oslo	-0.0103	-0.0098	-0.0086	
	(0.1443)	(0.1575)	(0.2034)	
S.Adj. Rain Stavanger	0.4380	0.4038	0.3745	
	(0.0299)	(0.0415)	(0.0607)	
S.Adj. Rain Tromsø	-0.0010	-0.0009	-0.0005	
	(0.2953)	(0.3216)	(0.4059)	
S.Adj. Rain Trondheim	0.6012	0.5940	0.3886	
	(0.0038)	(0.0033)	(0.0014)	
Log. Wind Prod.	-0.0109	-0.0108	-0.0104	-0.0111
	(0.0001)	(0.0001)	(0.0002)	(0.0002)

Sum Magazine Deviation	-0.0193	-0.0194	-0.0184	-0.0167
	(0.0000)	(0.0000)	(0.0000)	(0.0000)
Sum Sno., Gro., Sur. wtr.	-0.0073	-0.0073	-0.0074	-0.0071
	(0.0000)	(0.0000)	(0.0000)	(0.0000)
Dummy=1, 2020	-0.0477	-0.0468	-0.0538	-0.0365
	(0.3486)	(0.3582)	(0.2559)	(0.4406)
AR(1)	0.9387	0.9376	0.9421	0.9351
	(0.0000)	(0.0000)	(0.0000)	(0.0000)
MA(8)	0.0201			
	(0.4737)			
MA(11)	-0.0686	-0.0722	-0.0768	-0.0767
	(0.0008)	(0.0001)	(0.0001)	(0.0000)
MA(15)	-0.0089			
	(0.6407)			
MA(26)	-0.0504	-0.0562	-0.0560	-0.0680
	(0.0006)	(0.0001)	(0.0000)	(0.0000)
ARCH(1)	0.7412	0.7488	0.7081	0.6668
	(0.0000)	(0.0000)	(0.0000)	(0.0000)
GARCH(1)	0.4043	0.4008	0.4239	0.4508
	(0.0000)	(0.0000)	(0.0000)	(0.0000)
AIC	-2259.7211	-2262.9085	-2270.1139	-2246.7818
BIC	-2146.8162	-2159.0360	-2193.3386	-2170.0065
Log likelihood	1154.8605	1154.4542	1152.0570	1140.3909

Table 13: 0. AR(1)MA(8,11,15,26)-GARCH(1,1). 1. AR(1)MA(11,26)-GARCH(1,1). 2. AR(1)MA(11,26)-GARCH(1,1) No temp. 3. AR(1)MA(11,26)-GARCH(1,1) No rain. P-values in parenthesis.

B Population Weights

B.1 Population Weights

Year 2013 has been chosen, which is the middle of the data period. Data has been extracted from SSB[11].

B.1.1 Tables 14 to 16 and Equation B.1: Population Weights and Formula

Location	Population
Total Population (2013)	5051275
Oslo	623966
Bergen	267950
Stavanger	129191
Trondheim	179692
Tromsø	70358
Kristiansand	84476
Sum	1355633

Table 14: Population statistics for 2013.

Formula

$$\frac{\text{City Population}}{\text{Total Population}} = \text{Population Weight (total)}$$

$$\frac{\text{Total City Population}}{\text{City Population}} = \text{Population Weight (city in dataset)} \tag{B.1}$$

[11]Data can be found at SSB (2013), see table 57 and table 60.

Location	Weight
National Population (2013)	1
Oslo	0,123526436
Bergen	0,053046013
Stavanger	0,025575919
Trondheim	0,035573593
Tromsø	0,013928761
Kristiansand	0,016723698
Sum	0,26837442

Table 15: Population weights based on total population.

Location	Weight
Oslo	0,460276491
Bergen	0,19765674
Stavanger	0,095299392
Trondheim	0,132552099
Tromsø	0,051900477
Kristiansand	0,062314801
Sum	1

Table 16: Population weights based on dataset population.

C Descriptive Statistic Tables

C.1 Table 17: Variable Description for Variables in Dataset

Variable	Description
lnprice	Day-ahead logarithmic system price Nord Pool
rvar	Realized variance
lnwind_no	Logarithmic wind power production in Norway
magavvik_sum	Magazine Deviation from 20-year average
smg_sum	Sum snow, surface and groundwater
d2020	Dummy for 2020
swtp_brgc	Seasonally adj. and weighted temperature, Bergen
swtp_krsc	Seasonally adj. and weighted temperature, Kr.Sand
swtp_oslc	Seasonally adj. and weighted temperature, Oslo
swtp_troc	Seasonally adj. and weighted temperature, Tromsø
swtp_trd	Seasonally adj. and weighted temperature, Trondheim
swtp_stvgc	Seasonally adj. and weighted temperature, Stavanger
swrain_brgc	Seasonally adj. and weighted rainfall, Bergen
swrain_krsc	Seasonally adj. and weighted rainfall, Kr. Sand
swrain_oslc	Seasonally adj. and weighted rainfall, Oslo
swrain_stvgc	Seasonally adj. and weighted rainfall, Stavanger
swrain_troc	Seasonally adj. and weighted rainfall, Tromsø
swrain_trdc	Seasonally adj. and weighted rainfall, Trondheim

Table 17: Variables in dataset.

C.2 Table 18: Descriptive Statistics for Variables

Variable	Sum	Mean	SD	Min	Max	N
Realized variance	5.1809	0.0071	0.0294	0.0000	0.4897	727
Log. sys. Price	1098.45	1.50886	0.2474	0.2201	2.3036	728
Weekly sys. Price	26667.9500	36.6318	17.7646	1.6600	201.1900	728
Log. Wind Prod.	7752.7969	10.6494	0.9211	8.1261	12.9957	728
Temp. Bergen	6265.8365	8.6069	5.5599	-8.2429	22.7286	728
Rain Bergen	34993.4000	48.0679	43.2944	0.0000	255.8000	728
Temp. Kr.Sand	5739.7264	7.8951	6.6852	-13.7143	22.1429	728
Rain Kr.Sand	19418.9000	26.6743	27.8376	0.0000	178.0000	728
Temp. Oslo	5298.6237	7.2783	7.7659	-14.6286	23.9000	728
Rain Oslo	12423.1000	17.0647	17.5219	0.0000	86.5000	728
Temp. Stavanger	6292.7761	8.6677	5.5222	-9.4571	22.3286	728
Rain Stavanger	17453.5000	23.9746	21.2982	0.0000	122.8000	728
Temp. Tromsø	2599.4603	3.5707	6.0314	-10.6571	17.6714	728
Rain Tromsø	14680.0000	20.1648	18.7730	0.0000	102.7000	728
Temp. Trondheim	4428.1657	6.0826	6.6737	-14.4143	21.8714	728
Rain Trondheim	12157.6000	16.7000	16.3719	0.0000	95.6000	728
Sum Magazine Deviation	405.8659	0.5575	6.7613	-20.3078	16.7198	728
Sum Sno., Gro., Sur., wtr.	-23.7335	-0.0326	9.4112	-25.4913	41.2494	728
Dummy=1, 2020	52.0000	0.0713	0.2576	0.0000	1.0000	729

Table 18: Descriptive statistics for variables (no temperature and rain adjustment).

C.3 Table 19: Descriptive Statistics for Variables in ARIMA-GARCH

Variable	Sum	Mean	SD	Min	Max	N	Skewness
Realized Variance	5.1809	0.0071	0.0294	0.0000	0.4897	727	9.7795
Logarithmic System Price	1098.4501	1.5089	0.2474	0.2201	2.3036	728	-1.8290
Sum Mag. Dev.	405.8659	0.5575	6.7613	-20.3078	16.7198	728	-0.5424
Sum Sno, Gro, Sur. wtr.	-23.7335	-0.0326	9.4112	-25.4913	41.2494	728	0.8442
Dummy=1, 2020	52.0000	0.0713	0.2576	0.0000	1.0000	729	3.3311
S.Adj. Log Wind	134.1119	0.1984	0.4875	-1.2157	1.5599	676	-0.1317
S.Adj. Temp Bergen	-124.6242	-0.1844	2.9770	-11.1817	12.0957	676	0.2100
S.Adj. Temp Kristiansand	-1.0336	-0.0015	0.0800	-0.2681	0.2459	676	-0.0079
S.Adj. Temp Oslo	-3.4285	-0.0051	0.2181	-0.8360	0.6820	676	-0.0993
S.Adj. Temp Tromsø	0.3926	0.0006	0.0313	-0.1147	0.1236	676	-0.0382
S.Adj. Temp Trondheim	-28.2204	-0.0417	3.9174	-18.0612	18.1048	676	-0.1758
S.Adj. Temp Stavanger	3.5175	0.0052	0.3016	-1.2090	1.0183	676	0.0024
S.Adj. Rain Bergen	-0.1813	-0.0003	0.0424	-0.1652	0.1601	676	-0.1754
S.Adj. Rain Kr. Sand	-0.0488	-0.0001	0.0037	-0.0144	0.0133	676	-0.1750
S.Adj. Rain Oslo	-0.1697	-0.0003	0.1998	-0.5812	0.6660	676	-0.0373
S.Adj. Rain Stavanger	-0.1120	-0.0002	0.0108	-0.0378	0.0353	676	-0.0713
S.Adj. Rain Tromsø	-16.9645	-0.0251	1.9779	-6.7389	5.8793	676	-0.0596
S.Adj. Rain Trondheim	-4.8626	-0.0072	0.0906	-0.1960	0.2417	676	0.4459

Table 19: Descriptive statistics for variables used in ARIMA-GARCH estimation and postestimation (temperature and rain adjustment).

C.4 Table 20: Descriptive Statistics for Population Weights

Variables (No seasonal difference)	Weight	Mean	SD	Min	Max	N
Temperature Bergen	City	-0.0084	1.8539	-5.0385	8.1532	728
Rain Bergen	City	0.0754	0.0819	-0.1534	0.2506	728
Temperature Kr. Sand	City	0.0562	0.0579	0.0000	0.2859	728
Rain Kr.Sand	City	0.0089	0.0058	-0.0099	0.0233	728
Temperature Oslo	City	0.1833	0.1639	0.0000	0.9453	728
Rain Oslo	City	0.2003	0.3433	-0.6059	1.0047	728
Temperature Stavanger	City	0.2358	0.2208	0.0000	1.2090	728
Rain Stavanger	City	0.0147	0.0163	-0.0351	0.0533	728
Temperature Tromsø	City	0.0220	0.0217	0.0000	0.1269	728
Rain Tromsø	City	1.9129	1.5105	-1.2434	7.9631	728
Temperature Trondheim	City	4.8990	4.0933	0.0000	25.6549	728
Rain Trondheim	City	0.0026	0.0585	-0.1381	0.1651	728
Temperature Bergen	National	0.4528	0.2973	-0.4373	1.2057	728
Rain Bergen	National	2.5348	2.2939	0.0000	13.5692	728
Temperature Kr.Sand	National	0.1304	0.1130	-0.2294	0.3703	728
Rain Kr.Sand	National	0.4445	0.4646	0.0000	2.9768	728
Temperature Oslo	National	0.8877	0.9654	-1.8070	2.9523	728
Rain Oslo	National	2.1013	2.1625	0.0000	10.6850	728
Temperature Stavanger	National	0.2192	0.1429	-0.2419	0.5711	728
Rain Stavanger	National	0.6090	0.5445	0.0000	3.1407	728
Temperature Tromsø	National	0.0491	0.0841	-0.1484	0.2461	728
Rain Tromsø	National	0.2790	0.2613	0.0000	1.4305	728
Temperature Trondheim	National	0.2138	0.2384	-0.5128	0.7780	728
Rain Trondiem	National	0.5896	0.5821	0.0000	3.4008	728

Table 20: Descriptive statistics for population weighted weather. `City` indicates adjustment for dataset population and `National` indicates adjustment for national population.

D Unit Root Tests

D.1 Table 21: Philips-Perron Unit Root Test Results

Variable	P-value	τ	ρ	C ρ	C τ
(Log. sys. price)	(0.0011)	-4.0713	-34.0489	-14.1000	-2.8600
(S.Adj. Temp. Bergen)	(0.0036)	-3.7388	-27.8285	-14.1000	-2.8600
(S.Adj Temp. Kr. Sand)	(0.0000)	-23.7025	-618.0936	-14.1000	-2.8600
(S.Adj. Temp. Oslo)	(0.0000)	-22.0231	-603.6100	-14.1000	-2.8600
(S.Adj. Temp. Stavanger)	(0.0000)	-22.1202	-576.1667	-14.1000	-2.8600
(S.Adj. Temp. Trondheim)	(0.0000)	-14.5371	-325.8138	-14.1000	-2.8600
(S.Adj Temp. Tromsø)	(0.0000)	-22.7953	-620.7906	-14.1000	-2.8600
(S.Adj Rain Bergen)	(0.0000)	-5.3094	-54.5349	-14.1000	-2.8600
(S.Adj Rain Kr. Sand)	(0.0000)	-6.2579	-73.2116	-14.1000	-2.8600
(S.Adj Rain Oslo)	(0.0000)	-5.9628	-68.2447	-14.1000	-2.8600
(S.Adj Rain Stavanger)	(0.0000)	-6.6405	-82.5260	-14.1000	-2.8600
(S.Adj Rain Trondheim)	(0.0433)	-2.9179	-17.6915	-14.1000	-2.8600
(S.Adj Rain Tromsø)	(0.0000)	-19.5993	-564.2525	-14.1000	-2.8600
(Log. Wind. Prod)	(0.0001)	-4.8080	-43.5756	-14.1000	-2.8600
(Sum Sno,, Gro., Sur., wtr.)	(0.0016)	-3.9694	-31.4806	-14.1000	-2.8600
(Sum Magazine Deviation)	(0.0026)	-3.8282	-30.0552	-14.1000	-2.8600

Table 21: Philips-Perron unit root test results. 5% critical value.

D.2 Table 22: DF-GLS Test Results

Variable	N	L1τ	C L1	L2τ	C L2	L3τ	C L3
Log. System Price	724	-4.2501	-2.8641	-4.0983	-2.8623	-3.7354	-2.8604
S. Adj. Temp. Bergen	672	-4.0285	-2.8661	-4.1079	-2.8641	-4.3303	-2.8621
S. Adj. Temp. Kr. Sand	672	-14.0418	-2.8661	-10.7527	-2.8641	-8.9064	-2.8621
S. Adj. Temp. Oslo	672	-15.3764	-2.8661	-13.2395	-2.8641	-11.4268	-2.8621
S. Adj. Temp. Stavanger	672	-15.9740	-2.8661	-13.4188	-2.8641	-12.4325	-2.8621
S. Adj. Temp. Trondheim	672	-12.5682	-2.8661	-9.8432	-2.8641	-10.6233	-2.8621
S. Adj. Temp. Tromsø	672	-13.3058	-2.8661	-11.6167	-2.8641	-9.8538	-2.8621
S. Adj. Rain Bergen	672	-10.8274	-2.8661	-8.8329	-2.8641	-7.4633	-2.8621
S. Adj. Rain Kr. Sand	672	-11.8542	-2.8661	-9.4941	-2.8641	-7.7349	-2.8621
S. Adj. Rain Oslo	672	-10.1351	-2.8661	-7.4369	-2.8641	-5.7903	-2.8621
S. Adj. Rain Stavanger	672	-12.0951	-2.8661	-9.4228	-2.8641	-7.7888	-2.8621
S. Adj. Rain Trondheim	672	-2.8744	-2.8661	-2.9699	-2.8641	-3.1250	-2.8621
S. Adj. Rain Tromsø	672	-14.4443	-2.8661	-11.9911	-2.8641	-10.7778	-2.8621
Log. Wind. Prod	724	-5.1321	-2.8641	-4.0791	-2.8623	-3.1076	-2.8604
Sum Sno., Gro., and Sur., wtr.	724	-4.1877	-2.8641	-4.1751	-2.8623	-4.5311	-2.8604
Sum Magazine Deviation	724	-3.8592	-2.8641	-3.7787	-2.8623	-4.1459	-2.8604

Table 22: DF-GLS unit root test results. 5% critical value.

E ACF and PACF Plots

E.1 Figures 29 and 30: AR(1)MA(8,11,15,26)-GARCH ACF/-PACF

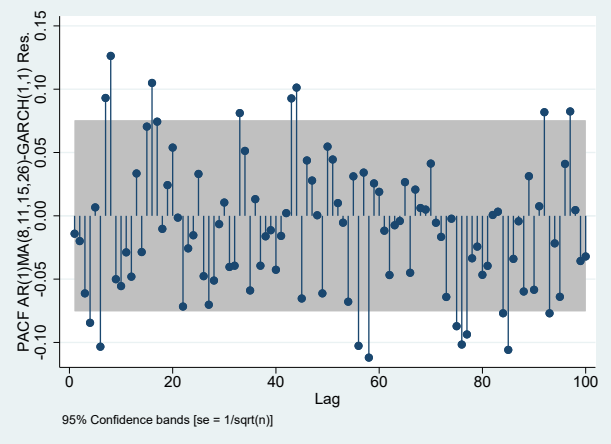

Figure 29: PACF ARIMA-GARCH.

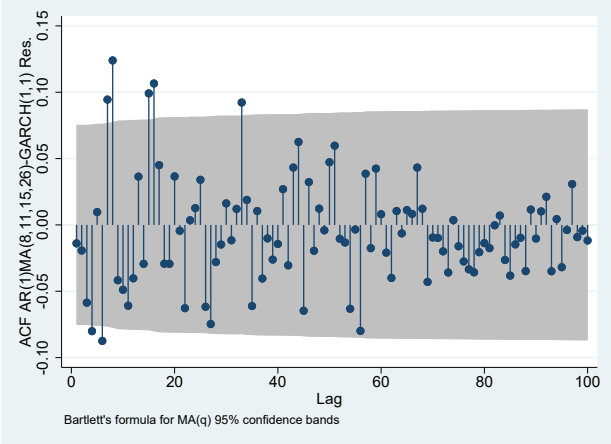

Figure 30: ACF ARIMA-GARCH.

E.2 Figures 31 and 32: AR(1)MA(11,26)-GARCH ACF/PACF

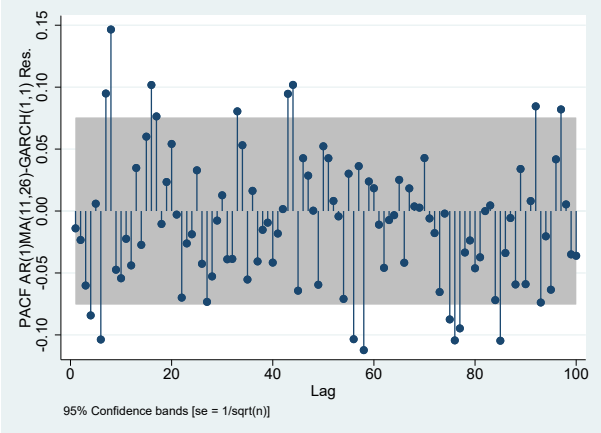

Figure 31: PACF ARIMA-GARCH.

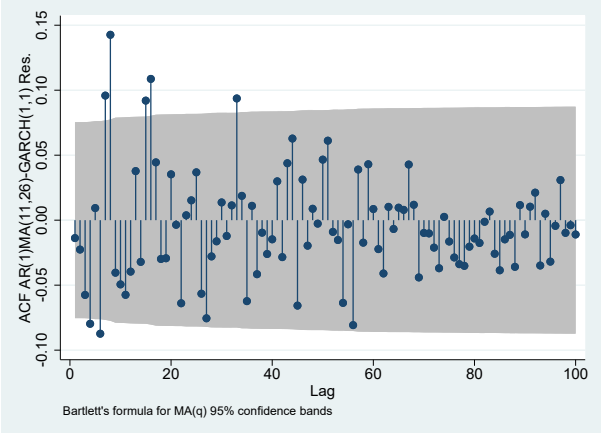

Figure 32: ACF ARIMA-GARCH.

E.3 Figures 33 and 34: AR(1)MA(11,26)-GARCH ACF/PACF

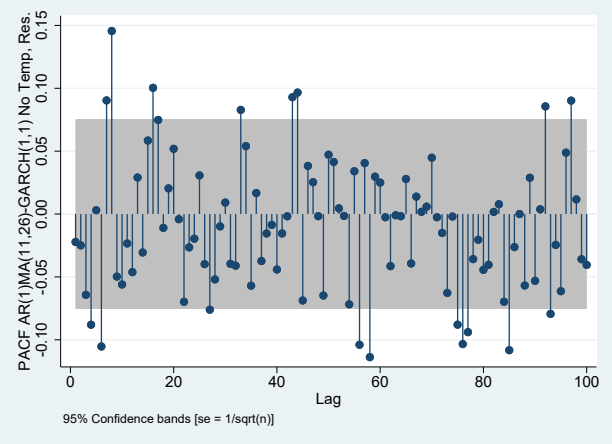

Figure 33: PACF ARIMA-GARCH No temp.

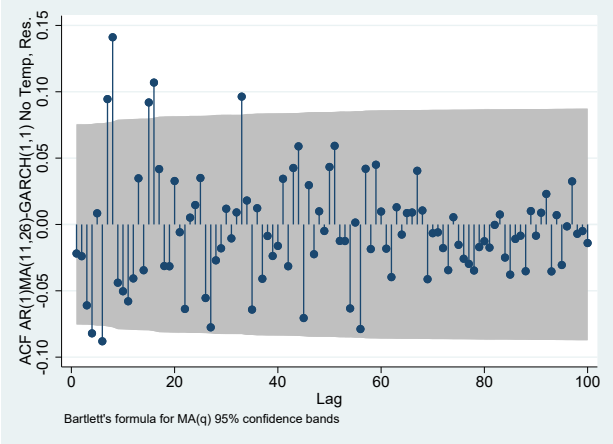

Figure 34: ACF ARIMA-GARCH No temp.

E.4 Figures 35 and 36: AR(1)MA(11,26)-GARCH ACF/PACF

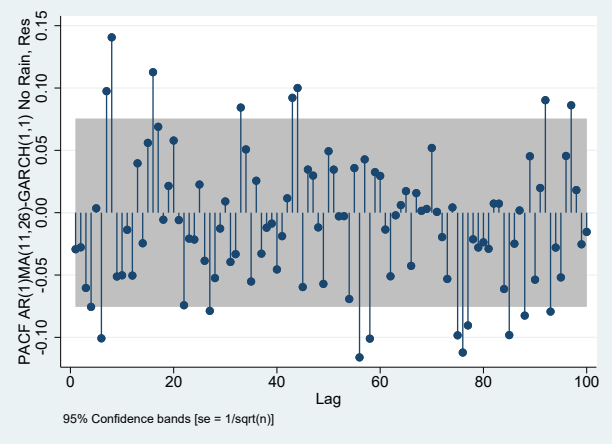

Figure 35: PACF ARIMA-GARCH No rain.

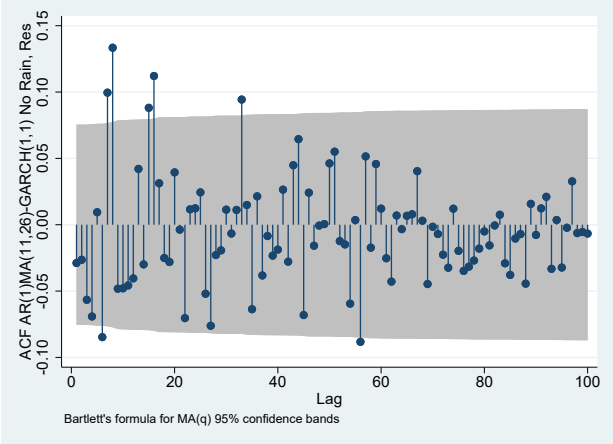

Figure 36: ACF ARIMA-GARCH No rain.

F ARIMA-GARCH Robustness

F.1 Table 23: Shapiro-Wilk Test Results

Variable	N	V	W	P-value	Z-stat
AR(1)MA(8,11,15,26)-GARCH(1,1)	676	102.0361	0.7691	0%	11.2674
AR(1)MA(11,26)-GARCH(1,1)	676	101.1419	0.7711	0%	11.2460
AR(1)MA(11,26)-GARCH(1,1) No T.	676	102.4251	0.7682	0%	11.2767
AR(1)MA(11,26)-GARCH(1,1) No R.	676	100.6095	0.7723	0%	11.2331

Table 23: Shapiro-Wilk test results.

F.2 Table 24 and Figures 37 to 40: Barlett's Periodogram Based Test

Variable	P-value	B-stat
AR(1)MA(8,11,15,26)-GARCH(1,1)	20.30%	1.0693
AR(1)MA(11,26)-GARCH(1,1)	17.76%	1.1001
AR(1)MA(11,26)-GARCH(1,1) No Temp	12.49%	1.1776
AR(1)MA(11,26)-GARCH(1,1) No Rain	11.31%	1.1984

Table 24: Barlett's periodogram bases test results.

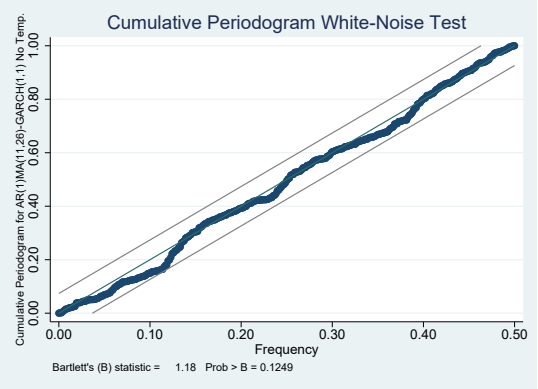

Figure 37: Barlett Periodogram for AR(1)MA(11,26)-GARCH(1,1) without temperature.

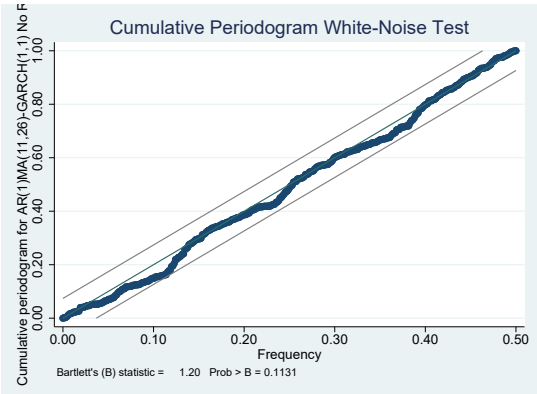

Figure 38: Barlett Periodogram for AR(1)MA(11,26)-GARCH(1,1) without rainfall.

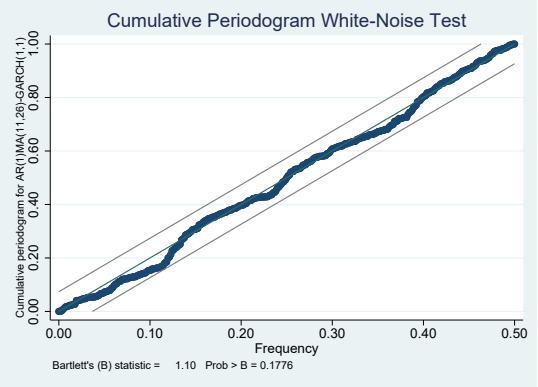

Figure 39: Barlett Periodogram for AR(1)MA(11,26)-GARCH(1,1).

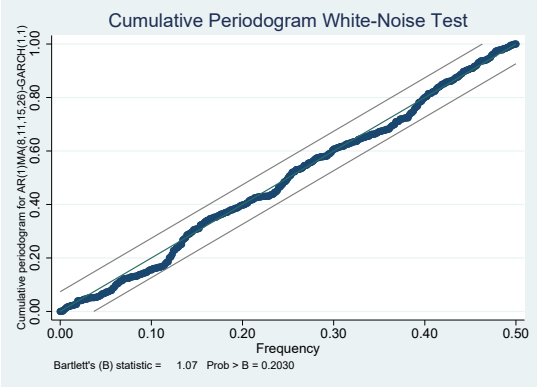

Figure 40: Barlett Periodogram for AR(1)MA(8,11,15,26)-GARCH(1,1).

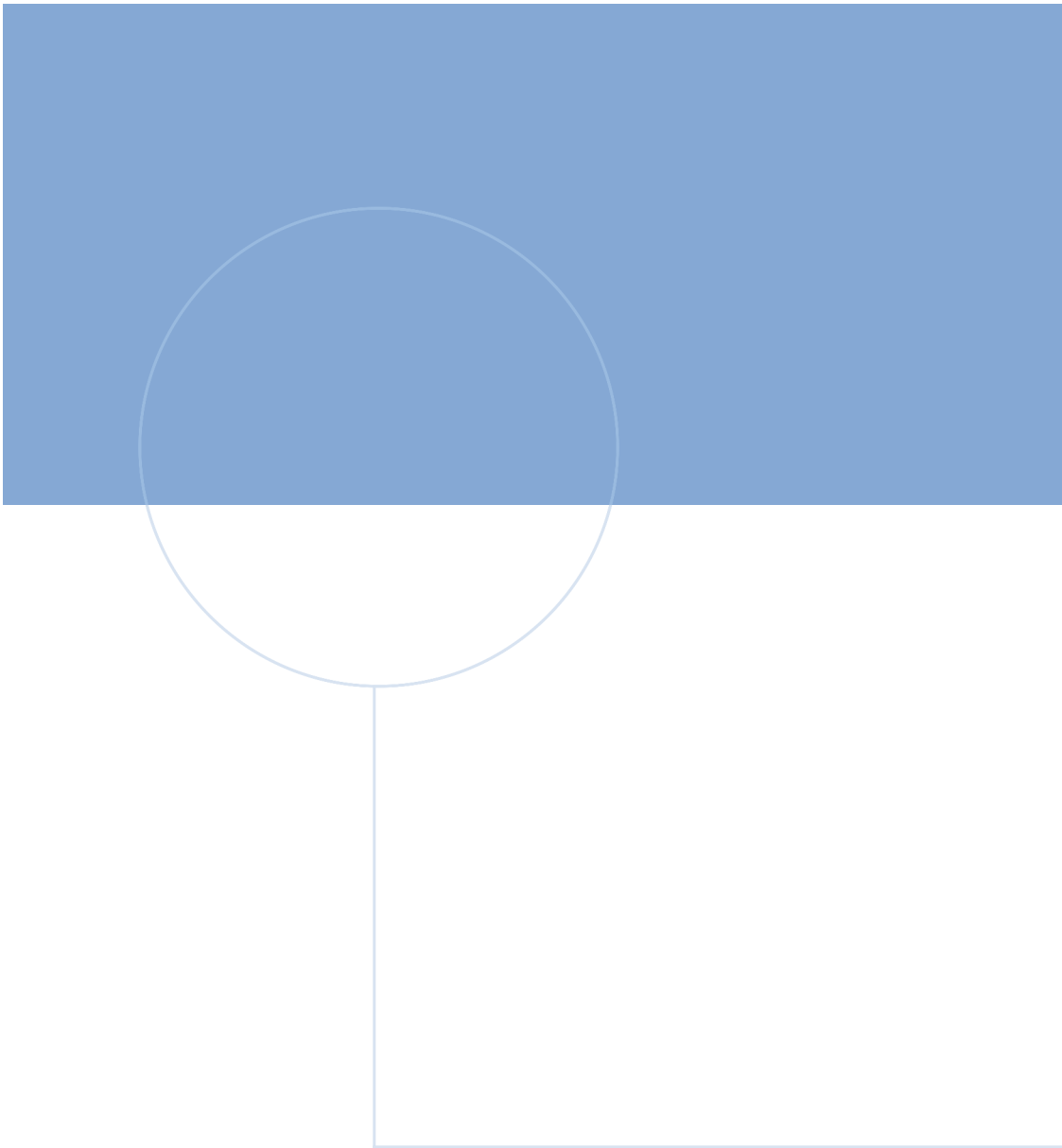

NTNU
Kunnskap for en bedre verden

DNV